Remote Sensing of Environment 280 (2022) 113195

Contents lists available at ScienceDirect

Remote Sensing of Environment

journal homepage: www.elsevier.com/locate/rse

Review

Fifty years of Landsat science and impacts

Michael A. Wulder [a,*], David P. Roy [b], Volker C. Radeloff [c], Thomas R. Loveland [d,1], Martha C. Anderson [e], David M. Johnson [f], Sean Healey [g], Zhe Zhu [h], Theodore A. Scambos [i], Nima Pahlevan [j,k], Matthew Hansen [l], Noel Gorelick [m], Christopher J. Crawford [d], Jeffrey G. Masek [n], Txomin Hermosilla [a], Joanne C. White [a], Alan S. Belward [o], Crystal Schaaf [p], Curtis E. Woodcock [q], Justin L. Huntington [r], Leo Lymburner [s], Patrick Hostert [t], Feng Gao [e], Alexei Lyapustin [u], Jean-Francois Pekel [o], Peter Strobl [o], Bruce D. Cook [n]

[a] Canadian Forest Service (Pacific Forestry Centre), Natural Resources Canada, 506 West Burnside Road, Victoria, British Columbia V8Z 1M5, Canada
[b] Department of Geography, Environment, & Spatial Sciences, Center for Global Change and Earth Observations, Michigan State University, USA
[c] SILVIS Lab, Department of Forest and Wildlife Ecology, University of Wisconsin-Madison, 1630 Linden Drive, Madison, WI 53706, USA
[d] U.S. Geological Survey Earth Resources Observation and Science (EROS) Center, 47914 252nd Street, Sioux Falls, SD 57198, USA
[e] USDA, Agricultural Research Service, Hydrology and Remote Sensing Laboratory, 10300 Baltimore Avenue, Beltsville, MD 20705, USA
[f] National Agricultural Statistics Service, United States Department of Agriculture, 1400 Independence Ave., SW, Washington, D.C. 20250, USA
[g] US Forest Service, Rocky Mountain Research Station, Ogden, UT 84401, USA
[h] Department of Natural Resources and the Environment, University of Connecticut, Storrs, CT 06269, United States
[i] Earth Science Observation Center, University of Colorado Boulder, Boulder, CO 80303, USA
[j] Science Systems and Applications, Inc., 10210 Greenbelt Rd., Lanham, MD 20706, USA
[k] Terrestrial Information Systems Laboratory, NASA Goddard Space Flight Center, Greenbelt, MD 20771, USA
[l] Department of Geographical Sciences, University of Maryland, College Park, MD 20740, USA
[m] Google Switzerland, Brandschenkestrasse 110, Zurich 8002, Switzerland
[n] Biospheric Sciences Laboratory, NASA Goddard Space Flight Center, Greenbelt, MD 20771, USA
[o] European Commission, Joint Research Centre, 21027 Ispra, Italy
[p] School for the Environment, University of Massachusetts Boston, 100 Morrissey Blvd, Boston, MA 02125, USA
[q] Department of Earth and Environment, Boston University, MA 02215, USA
[r] Desert Research Institute, Reno, NV 89512, USA
[s] Geoscience Australia, GPO Box 378, Canberra, ACT 2601, Australia
[t] Geography Department, Humboldt-Universität zu Berlin, Unter den Linden 6, 10099 Berlin, Germany
[u] Laboratory for Atmospheres, NASA Goddard Space Flight Center, Greenbelt, MD, USA

ARTICLE INFO

Edited by Dr Marie Weiss

Keywords:
Earth observation
Land cover
Land use
Climate change
Human footprint
Open data
Satellite

ABSTRACT

Since 1972, the Landsat program has been continually monitoring the Earth, to now provide 50 years of digital, multispectral, medium spatial resolution observations. Over this time, Landsat data were crucial for many scientific and technical advances. Prior to the Landsat program, detailed, synoptic depictions of the Earth's surface were rare, and the ability to acquire and work with large datasets was limited. The early years of the Landsat program delivered a series of technological breakthroughs, pioneering new methods, and demonstrating the ability and capacity of digital satellite imagery, creating a template for other global Earth observation missions and programs. Innovations driven by the Landsat program have paved the way for subsequent science, application, and policy support activities. The economic and scientific value of the knowledge gained through the Landsat program has been long recognized, and despite periods of funding uncertainty, has resulted in the program's 50 years of continuity, as well as substantive and ongoing improvements to payload and mission performance. Free and open access to Landsat data, enacted in 2008, was unprecedented for medium spatial resolution Earth observation data and substantially increased usage and led to a proliferation of science and application opportunities. Here, we highlight key developments over the past 50 years of the Landsat program that have influenced and changed our scientific understanding of the Earth system. Major scientific and programmatic impacts have been realized in the areas of agricultural crop mapping and water use, climate change

* Corresponding author.
E-mail address: mike.wulder@nrcan-rncan.gc.ca (M.A. Wulder).
[1] Deceased May 13, 2022

https://doi.org/10.1016/j.rse.2022.113195
Received 7 April 2022; Received in revised form 19 July 2022; Accepted 21 July 2022
Available online 28 July 2022

drivers and impacts, ecosystems and land cover monitoring, and mapping the changing human footprint. The introduction of Landsat collection processing, coupled with the free and open data policy, facilitated a transition in Landsat data usage away from single images and towards time series analyses over large areas and has fostered the widespread use of science-grade data. The launch of Landsat-9 on September 27, 2021, and the advanced planning of its successor mission, Landsat-Next, underscore the sustained institutional support for the program. Such support and commitment to continuity is recognition of both the historic impact the program, and the future potential to build upon Landsat's remarkable 50-year legacy.

1. Introduction

The successful September 27, 2021, launch of the National Aeronautics and Space Administration (NASA)/United States Geological Survey (USGS) Landsat-9 Earth observation (EO) mission secured the continuity of the longest global environmental satellite record (Masek et al., 2020), which now spans five decades since the July 1972 launch of Landsat-1 (Goward et al., 2021). In that period, the human population has doubled (OECD, 2020), and the understanding of humanity's direct and indirect role in modifying the environment and climate has evolved from research to widespread concern along with growing political commitments to redress anthropogenic impacts (IPCC, 2021). Currently, Landsat-9, together with Landsat-8, provide 8-day global 30-m multispectral data coverage that is used to monitor, understand, and manage the Earth's resources and terrestrial processes (Table 1) (Masek et al., 2020; Roy et al., 2014b; Wulder et al., 2019). The combination of data

Table 1
Summary of key dates of Landsat program and evolving sensor and technical characteristics.

Landsat Satellite	Launch - Lifespan	Sensors[1,2]	Spectral[3] (spatial) resolution	Radiometric resolution (bits)	Onboard science data storage[4]	Science data transfer rate (Mbps)[4]	Approximate number of scenes/day[4]	Orbital altitude and scene reference system[3]
1	July 23, 1972 to January 6, 1978	MSS	4 VISNIR (80 m; 79-m pixels based on a 57 × 79 m ground sampling distance; noting, also often resampled to 60 m)	6	Wideband video tape recorder (3.4 GB capacity)	15	147 (best year, average)	917 km WRS-1
2	January 22, 1975 to February 25, 1982 (officially decommissioned: July 27, 1983)	MSS	4 VISNIR (80 m)	6	Wideband video tape recorder (3.4 GB capacity)	15	122 (best year, average)	917 km WRS-1
3	March 5, 1978 to March of 1983 (officially decommissioned: September 7, 1983)	MSS	4 VISNIR (80 m) (had a 240 m TIR channel, but failed shortly after launch)	6	Wideband video tape recorder (3.4 GB capacity)	15	70 (best year, average)	917 km WRS-1
4	July 16, 1982 to December 14, 1993 (officially decommissioned: June 15, 2001)	MSS TM	MSS (as above) 4 VISNIR (30 m) 2 SWIR (30 m) 1 TIR (120 m)	MSS: 6; TM: 8	None	85	50 (best year, average)	705 km WRS-2
5	March 1, 1984 to January 2013 (officially decommissioned: June 19, 2013)	MSS TM	MSS (as above) 4 VISNIR (30 m) 2 SWIR (30 m) 1 TIR (120 m)	MSS: 6; TM: 8	None	85	147 (best year, average); 50–140 from 1993 forward	705 km WRS-2
6	October 5, 1993 (failed to achieve orbit)	ETM	1 PAN (15 m) 4 VISNIR (30 m) 2 SWIR (30 m) 1 TIR (120 m)	8	NA	NA	NA	705 km WRS-2
7	April 15, 1999 to present	ETM+	1 PAN (15 m) 4 VISNIR (30 m) 2 SWIR (30 m) TIR (60 m; with high and low gain settings)	8	Solid state recorder (47 GB capacity)	150	550 (current rate; fewer in previous periods)	705 km WRS-2
8	February 11, 2013 to present	OLI TIRS	1 PAN (15 m) 4 VISNIR (30 m) 2 Coastal Aerosol/Cirrus (30 m) 2 SWIR (30 m) 2 TIR (100 m)	12	Solid state recorder (400 GB capacity)	384	740	705 km WRS-2
9	September 27, 2021 to present	OLI-2 TIRS-2	1 PAN (15 m) 4 VISNIR (30 m) 2 Coastal Aerosol/Cirrus (30 m) 2 SWIR (30 m) 2 TIR (100 m)	14	Solid state recorder (4 TB capacity)	384	740	705 km WRS-2

[1] Landsats 1 to 3 all carried the Return Beam Vidicon (RBV).
[2] MSS: Multispectral Scanner System (official) or Multispectral Scanner (common usage); TM: Thematic Mapper; ETM: Enhanced Thematic Mapper; ETM+: Enhanced Thematic Mapper Plus; OLI: Operational Land Imager; TIRS: Thermal Infrared Sensor.
[3] VISNIR: visible, near infrared; PAN: panchromatic; SWIR: shortwave infrared; TIR: thermal infrared; WRS: Worldwide Reference System.
[4] Numbers drawn from Goward et al. (2017), Markham et al. (2018), Roy et al. (2014a), and Masek et al. (2020).

from the eight successful Landsat missions provides the foremost global environmental baseline against which we can contextualize detected change at scales of human influence. Free and open EO data, coupled with advances in internet, cloud computing, and open-source software are broadening applications and have reduced barriers to access (Wulder and Coops, 2014).

Transparent environmental monitoring in support of national programs and reporting linked to multilateral agreements are being enabled by the increasingly automated extraction of actionable information from satellite time series, underscoring the importance of science-quality observations and systematic acquisitions (Roy et al., 2014b). NASA is responsible for the design and launch of the Landsat satellites, with operations, data archiving, calibration, and distribution undertaken by the USGS. The USGS has set the benchmark for rigorous cross-calibration, and reprocessing to ensure continuous availability of calibrated observations, all of which are freely and openly distributed. This includes state-of-the-art data management for current missions as well as recovery and gathering of data from international archives (Wulder et al., 2016). The US Sustainable Land Imaging Program will build on the Landsat record for at least another decade, with development of a successor to Landsat-9, the Landsat-Next mission (Masek et al., 2020), already approved, with planned advances to spatial, spectral, temporal, and radiometric resolutions as well as changes to the satellite architecture.

The history of the Landsat program has been described in detail by past and current members of the USGS-NASA Landsat Science Team (see Goward et al., 2017, 2021; Roy et al., 2014b; Wulder et al., 2019); herein, we share key scientific and programmatic impacts associated with the first 50 years of the Landsat program. These impacts span the life of the program to date and exemplify the varying information interests of the different eras, as well as demonstrating how impacts resulted in further investments in the program and increased science and application capacity over time. The thematic achievement areas identified are: agricultural crop mapping and water use, climate change drivers and impacts, ecosystem and land cover monitoring, and anthropogenic impacts, underpinned by science-grade, free and open data and open science.

2. Landsat utilization and uptake

2.1. Landsat science-grade data generation

In the early years of the Landsat program users typically worked with single cloud-free images. The introduction of Landsat collection-based processing has ensured the provision of science-grade, consistently processed data needed for time series analyses. In September 2016, the USGS initiated the first reprocessing of the US Landsat archive, termed Collection 1, using the most up-to-date radiometric calibration and geolocation information (Dwyer et al., 2018). In September 2020, the USGS finished the second reprocessing, termed Collection 2, that was driven primarily by the availability of globally improved geolocation information (Storey et al., 2019) and was strategically scheduled to ensure that the Landsat-9 data were processed consistently with the Landsat-1 to -8 data for Collection 2. The successful Moderate Resolution Imaging Spectroradiometer (MODIS) land product generation approach demonstrated the utility of periodic collection-based reprocessing to accommodate improved sensor characterization and algorithms (Justice et al., 2002). Prior to the Landsat collection-based processing, users could order the same Landsat image on different dates, and the data provided to them could differ as a result of changes in the calibration and geolocation information used in the USGS Landsat processing system. Collection-based processing is therefore fundamental for consistent pre-processed science-grade data, and is also useful for providing scientific provenance, noting the criticality of trust by the broader community is dependent on traceable/reproducible workflows and well-documented data pre-processing protocols (Roy et al., 2014b; Tulbure et al., 2021).

Radiometric calibration and precise geolocation of satellite imagery are fundamental pre-processing steps. Since the inception of the Landsat program, all Landsat instruments have undergone pre-launch characterization so that (i) the recorded digital numbers can be converted into physically meaningful top of atmosphere (TOA) radiance, and (ii) the sensed data can be geolocated accurately (Barsi et al., 2014; Markham and Helder, 2012; Storey et al., 2014). Pre-launch characterization is supplemented by onboard devices used to conduct on-orbit assessment and to monitor instrument stability and performance. The Landsat-8 and -9 sensors have fully operational global position systems and the USGS processes all the archive to the best achievable geolocation accuracy, either as L1GS (systematically corrected using satellite ephemeris information), L1GT (systematically corrected with relief distortion correction using digital elevation data), or L1TP (precision and terrain corrected) (Yan and Roy, 2021). The L1TP provides the highest accuracy and is achieved by image matching with a ground control chip library (Storey et al., 2019) that has recently been supplemented using European Space Agency (ESA) Sentinel-2 image subsets (Gascon et al., 2017). For user convenience, the Landsat images are categorized as Tier 1 if they have a geolocation root-mean-squared error (RMSE) $\leq$12 m or as Tier 2 if they do not.

It is well established that the atmosphere can significantly influence TOA reflectance (Fraser and Kaufman, 1985) and that atmospheric correction of Landsat TOA reflectance to land surface reflectance (and to aquatic reflectance) is required for reliable surface monitoring (Gordon and Clark, 1981; Masek et al., 2006). For example, the mean absolute difference between TOA reflectance and land surface reflectance, expressed as a percentage of land surface reflectance, was documented as 45%, 22%, and 12% for the Landsat Enhanced Thematic Mapper Plus (ETM+) blue, green, and red bands across the United States, respectively (Roy et al., 2014a). In recognition of the need for systematically generated atmospherically corrected Landsat imagery, the USGS started to provide TOA and surface reflectance Landsat Analysis Ready Data (ARD) (Dwyer et al., 2018). Now Landsat surface reflectance and surface temperature are generated systematically on a global basis using a combined radiative transfer and image content approach (Malakar et al., 2018; Vermote et al., 2015) for Collection 2 for all of the Landsat 30-m image data in the archive. Similarly, provisional aquatic reflectance products from Landsat-8 observations are also available on-demand via USGS Earth Resources Observation and Science (EROS) Science Processing Architecture (ESPA) (Franz et al., 2015; Pahlevan et al., 2017). The Landsat ARD are provided in fixed non-overlapping tiles over the conterminous United States (CONUS) plus Alaska and Hawaii, defined in the Albers Equal Area projection, and are designed to make it significantly easier for users to compare Landsat observations through time and space (Dwyer et al., 2018). The Landsat ARD are derived using Tier-1 data to ensure “stackable” well-geolocated data needed for time series analyses. An important element of the ARD is per-pixel quality flags, and associated metadata, that allow users to set criteria for data selection, such as the removal of saturated pixels or pixels that are obscured by cloud, haze, smoke, or shadows.

The above noted geometric and radiometric processing is essential to ensure a seamless multi-sensor data record where observed satellite changes can be ascribed to surface changes and not to instrument changes (Cohen et al., 2016; Markham and Helder, 2012). Other factors, such as spectral band pass differences between Landsat sensor generations (Holden and Woodcock, 2016; Roy et al., 2016a), bi-directional reflectance variations associated with changing view and solar geometry (Roy et al., 2016b), and orbit drift in the 26-year Landsat-5 record (Zhang and Roy, 2016) and the last few years of Landsat-7 (Qiu et al., 2021) are subject to ongoing research and their normalization is not yet implemented in the USGS Landsat processing.

The later Landsat missions offer improved spectral coverage to allow for better compensation of atmospheric effects (e.g., absorbing aerosols, haze, thin clouds, cloud shadows) in both the solar reflective and

thermal bands. The emergence of machine-learning-based atmospheric correction methods (Pahlevan et al., 2021; Skakun et al., 2022) will increase user confidence in the decision-making frameworks for expedited services (e.g. wildfire detection and characterization) as well as in scientific time series analyses. An additional enhancement with Collection 2 is the ability to convert well-calibrated TOA brightness temperatures from single and dual thermal infrared spectral bands on Landsats 4–9 to generate atmospherically corrected surface temperature products (Cook et al., 2014; Masek et al., 2020). This algorithmic advancement leveraged decades of Landsat thermal infrared research and development regarding both radiative transfer (Laraby and Schott, 2018; Malakar et al., 2018) and measurement-modeling split-window techniques (Gerace et al., 2020) to compensate for atmospheric effects and incorporate surface emissivity measures available through the ASTER Global Emissivity Database (GED) (Hulley et al., 2015).

Based on a strong partnership between NASA, USGS, ESA, and the European Union's Copernicus program, the systematic production of harmonized Landsat-8 and Sentinel-2 observational record is in place. The Sentinel-2 MultiSpectral Instrument (MSI) provides 10–20-m multispectral observations (Drusch et al., 2012) with wavelengths similar to the Landsat-8 Operational Land Imager (OLI). The NASA Harmonized Landsat Sentinel-2 (HLS; available at: https://lpdaac.usgs.gov/) effort harmonizes the Sentinel-2A and -2B observations to Landsat-8 to provide a precisely geometrically co-registered and spectrally-consistent 30-m products. In brief, the HLS processing addresses cross-sensor differences in spectral band passes and spatial resolution, and also accommodates data projection and tiling requirements (Claverie et al., 2018). Due to differing orbital tracks and swath dimensions (Roy et al., 2017), the HLS products also have a Nadir Bidirectional Reflectance Distribution Function (BRDF) Adjusted Reflectance (NBAR) correction applied to reduce bi-directional reflectance view angle variations (Claverie et al., 2018; Roy et al., 2016b). Operating as a virtual constellation (Wulder et al., 2015), harmonization with data from the Copernicus Sentinel-2 mission has reduced Landsat's effective revisit interval (non-thermal bands) from weeks to days. While varying by latitude, the combination of Landsat-8 and Sentinel-2A and -2B, provides an observation opportunity every 2–4 days, with a global median average revisit interval of 2.9 days (Li and Roy, 2017). Introducing Landsat-9 observations will further enhance such harmonization activities, with an observation from the four-satellite constellation with an expected global median revisit of 2.3 days (Li and Chen, 2020).

2.2. Landsat data access and open science

One of the most significant developments over the past 50 years of the Landsat program has been the adoption of a free and open data policy. Historically, when Landsat data were first available, data were provided on physical media at the marginal cost of reproduction and dissemination. This cost was typically borne by the user or by an agency working on the behalf of users, with costs ranging from $20 (US dollars) for an individual photographic image (1972–1978) to $200 for digital data (1979–1982). Over time and through various changes in programmatic and agency responsibilities, including the Landsat Commercialization Act of 1984 that resulted in a period of public-private partnership (Hufbauer, 1991; Marshall, 1989), increased fee structures emerged. While dependent upon era, for much of 1983–1998, costs per image ranged from ~$3000 to $4000. At the time of the Landsat-7 launch in April 1999, each image cost ~$2500, which dropped to $600 by the end of 1999 (for details, see Goward et al., 2017; Wulder et al., 2012).

In October 2008, the USGS implemented a policy to provide the US-held contents of the Landsat archive at no cost to anyone via the internet (Woodcock et al., 2008). The Landsat free and open data distribution policy was unprecedented for medium spatial resolution data. Following this policy change, all images outside of the core archive (i.e. data held by the global receiving station network) were identified and provided to the USGS through the Landsat Global Archive Consolidation initiative (Wulder et al., 2016). Except for countries that, at that time, had limited internet bandwidth and a continued reliance on physical media distribution (Roy et al., 2010), the free and open data policy made the archive accessible to the global user community. Notably, the data from other global coverage remote sensing systems such as the National Oceanic and Atmospheric Administration (NOAA) Advanced Very High-Resolution Radiometer (AVHRR), available since 1979 (Cracknell, 2001), and the NASA MODIS, available since 2000 (Justice et al., 1998), have always been freely available; however, these data have a significantly coarser spatial resolution than Landsat. Consequently, prior to the 2008 opening of the Landsat archive, many remote sensing users gravitated to coarse spatial resolution data because the data were free, and when Landsat images were used, they were used judiciously due to their cost (Goward et al., 2017).

Free and open Landsat access was a true paradigm change for medium spatial resolution satellite remote sensing, the implications of which are still being realized (Zhu et al., 2019a). For society to benefit from investments in EO, making those data readily available in a useable form serves to broaden the use of the data and the range of possible insights to be made. Not only did the free and open data policy expand data utilization, it also increased the depth and scope of the science questions asked and applications undertaken. Concurrent with the free and open data policy, collection-based processing, and analysis ready data improvements, have been increases in data storage and processing capacity. Data can be downloaded for local processing on workstations or high-performance computing clusters, or can be directly accessed and analyzed on commercial cloud computing platforms (e.g., as developed by Google, Amazon, or Microsoft, among others). As a consequence, there is now a hierarchy of services offered with satellite data, computing, software, and information products as services. Open access and open source code practices have been driving Landsat uptake across a wide range of sectors (Giuliani et al., 2017). Today, open data sharing policies and practices are a recognised success of the international Group on Earth Observations, underpinning its Global Earth Observation System of Systems (Doldirina, 2015). A challenge associated with easy-to-produce continental-global scale products, is the capacity to validate products at that scale (Tulbure et al., 2021).

A particular development that has helped incentivize the broad adoption and uptake of Landsat data was the release of Google Earth Engine, a cloud-based platform for large-scale data analysis that is free to use for research and non-commercial purposes (Gorelick et al., 2017). Development on Google Earth Engine began concurrently with the opening of the Landsat archive in 2008, and was publicly launched in 2012, mirroring a copy of the Landsat public archive hosted by the USGS. Today, Google Earth Engine maintains online copies of more than 600 different EO and ancillary datasets, totalling more than 50 petabytes. Having all these data in one easy-to-use system, co-located with significant computational power, has made Google Earth Engine a popular platform for researchers, with more than 500,000 users registered (as of January 2022) from more than 250 countries and territories. The Landsat data hosted within Google Earth Engine include the different Landsat collections categorized by sensor, the processing level (i.e. Tier 1 or Tier 2), and the product (e.g. surface or TOA reflectance). Recent usage statistics reveal that upwards of 10,000 distinct users make use of the Landsat-8, Collection 1, Tier 1, surface reflectance (LC08/C1/T1_SR) collection weekly, and together, all of the Landsat collections are used by around 40,000 users per week (Fig. 1). This notable uptake has translated into a wealth of scientific publications with Earth Engine and Landsat being mentioned together in approximately 14,000 document records ("Landsat AND "Earth Engine"", Google Scholar; March 9, 2022).

2.3. Landsat science and application activity

Based on the number of published works, the Landsat program made

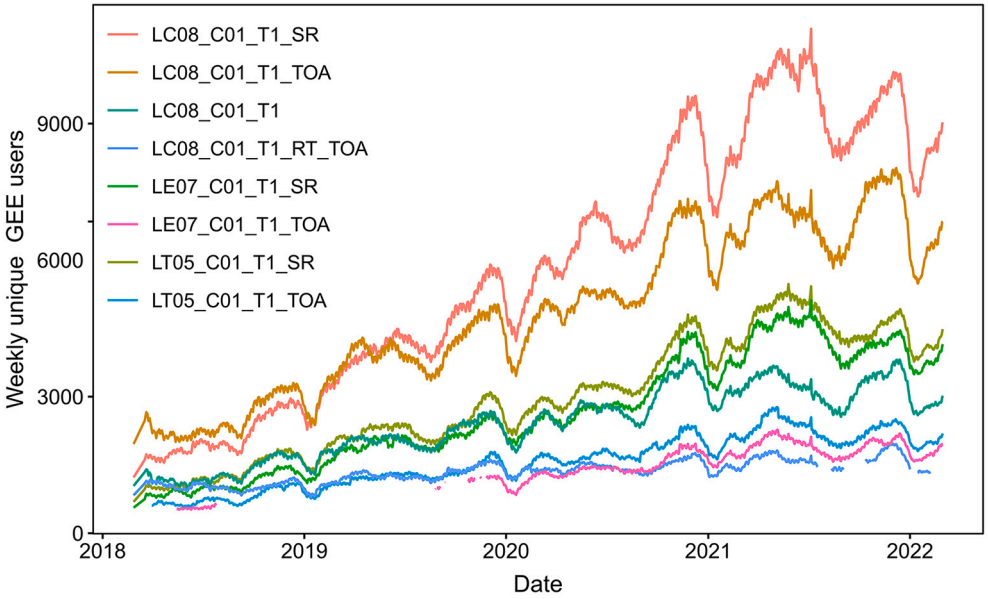

Fig. 1. Summary of usage of redistributed Landsat Collection 1 data on Google Earth Engine, by collection and product traits. Legend codes denote the Landsat sensor, collection number (C), processing tier (T), and product (SR, surface reflectance; TOA, top of atmosphere).

a larger scientific contribution than any other EO satellite program (Fig. 2). As of February 2022, there were 767,000 publication records in Google Scholar listed with the keyword Landsat, which is 1.5 times greater than the number of references for MODIS, 5.5 times greater than AVHRR, 7.5 times greater than SRTM, 7.4 times greater than ERS-1, and at least one order of magnitude greater than the number of published scientific works from any other comparable EO program. For comparison, using more stringent inclusion criteria, over 35,000 published works are listed in the Web of Science with the keyword Landsat, having a similar ranking relative to the sensors as listed above. These statistics demonstrate unambiguously that no other EO satellite program has dominated the scientific literature the way Landsat has, and continues to do.

Indeed, Landsat has dominated the scientific literature since the program's inception (Fig. 3), despite the availability of other open access EO data sources, such as MODIS since 1999. Until 1999, the number of references per year according to Google Scholar never exceeded 5000, compared to the peak of 31,800 in 2019. Accordingly, only 15% of Landsat references were published prior to the MODIS launch, and 25% prior to the 2015 Sentinel-2 launch. The dominance of Landsat among EO satellite programs is especially notable given that the data had to be purchased for most of its history (Wulder et al., 2012). In addition, until recently there were very few ready-to-use products from Landsat data, unlike the suite of MODIS land products that were openly available to the community, which allowed non-remote sensing specialists to utilize MODIS data more readily (Justice et al., 2002).

Landsat data have made important contributions to many different science and application areas (Fig. 4). According to key words and research categories in the Web of Science, there are 11,465 (~35%) Landsat papers related to “land cover or land use”, followed by 6108

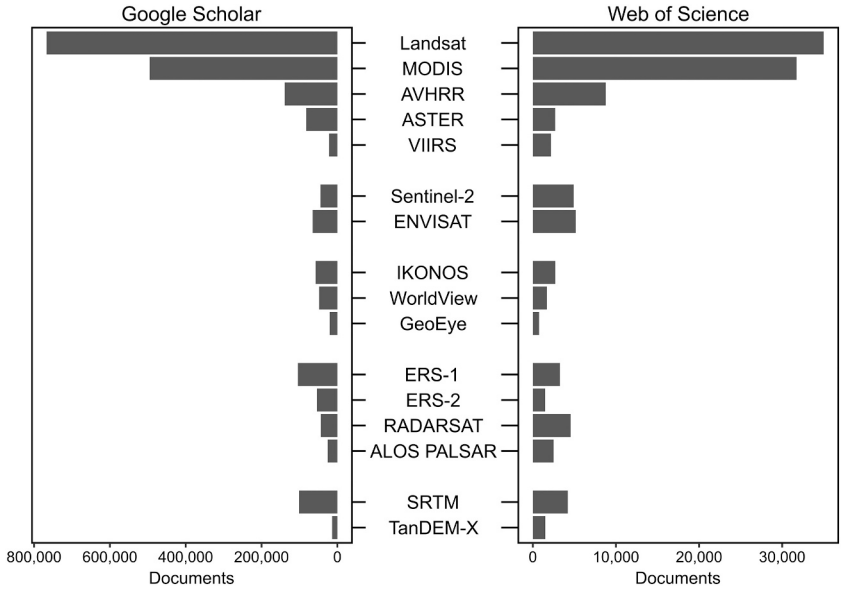

Fig. 2. Number of document records for different satellites according to Google Scholar (left), and the Web of Science (right).”ASTER” required the additional keyword”satellite” to remove erroneous selections. Both “SPOT” and “SPOT and satellite” resulted in numerous erroneous selections, which is why this sensor is not included. (Searched Feb. 14, 2022).

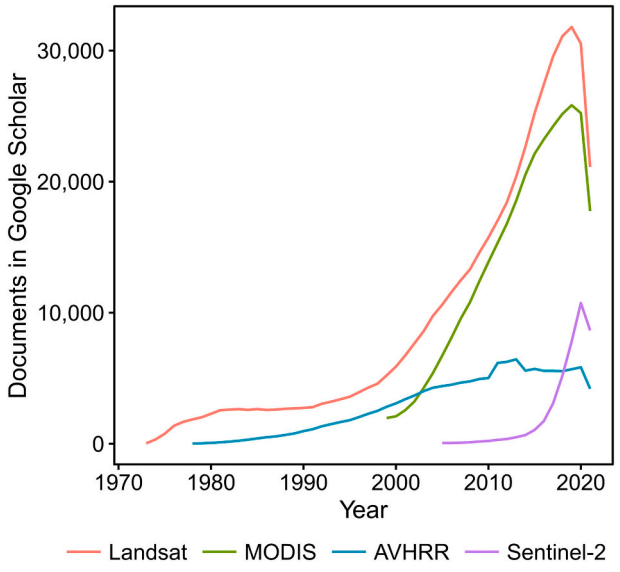

Fig. 3. Number of document records associated with the four major optical Earth observation satellites according to Google Scholar from 1972 to 2021 (Searched Feb. 14, 2022). For visualization purposes, we show the three-year rolling average.

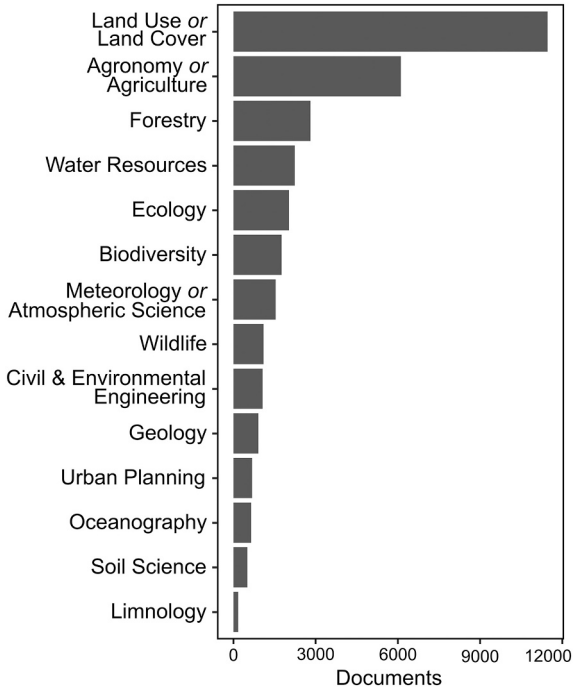

Fig. 4. Number of document records for published works in Web of Science for different application areas. Numbers obtained from the Web of Science research category, or for a search for Landsat AND the keyword (as found on the y-axis) and noted here whichever was larger (Searched February 14, 2022).

(18%) for "agronomy or agriculture", the subject areas that Landsat was initially envisioned for, and 2810 (9%) for "forestry". "water resources" (7%), "ecology" (6%), "biodiversity" (5%), and "meteorology or atmospheric science" (5%) follow in emphasis. These different applications areas highlight the usefulness of Landsat data in a wide range of scientific disciplines and for many land and water applications and management questions. When interpreting bibliometrics regarding numbers of published articles and related citations, it is prudent to recall the increase in the overall number of journals publishing on remote sensing topics and the concurrent rise in citations.

Analysis of the top-50 most-cited papers that have used the keyword Landsat provides further indication of Landsat's contributions to science. We highlight here the impacts from a sample of these top-cited Landsat papers. Landsat data played a primary role in all selected papers. Topping the list by a notable margin is the paper by Hansen et al. (2013) on 21st century global forest change with 8100 citations in Google Scholar, and 5300 in Web of Science. Indeed, highlighting the rapid rates of forest canopy cover change, especially in the tropics, has been a major contribution of Landsat to science (Gibbs et al., 2007, 2010; Kennedy et al., 2010; Skole and Tucker, 1993). An additional important scientific contribution has been the identification of urban heat islands, made uniquely possible by Landsat's thermal sensors (Chen et al., 2006; Weng et al., 2004; Yuan and Bauer, 2007). Another group of papers made important contributions by providing baseline data for subsequent studies, such as land cover classifications (Chen et al., 2014; Gong et al., 2013; Homer et al., 2004; Vogelmann et al., 2001), global surface water mapping (Pekel et al., 2016), land use change maps (Liu et al., 2014), and global mangrove maps (Giri et al., 2011). Similarly, there are crucial papers that either fused Landsat with data from other sensors (Chavez et al., 1991; Gao et al., 2006; Nunez et al., 1999), or utilized Landsat to validate coarser spatial resolution satellite products maps (Friedl et al., 2002). Lastly, there are foundational papers that examined the performance of vegetation and water indices (Huete et al., 1997; Xu, 2006), calibration coefficients (Chander et al., 2009), atmospheric correction (Masek et al., 2006; Song et al., 2001), cloud masking (Zhu et al., 2015; Zhu and Woodcock, 2012), and the impact of the opening of the Landsat archive (Wulder et al., 2012). The wide range of topics in the top-50 list reflects the diverse contribution of the Landsat program to science: from facilitating the direct testing of hypotheses and the provision of ready-to-use datasets, to the development of the image pre-processing algorithms that are required for the illustrated scientific contributions.

The demonstrated ability of Landsat to capture information over a wide range of attributes with management or policy implications led to institutional interest in expanded use of satellite data (Wulder et al., 2019). This has occurred at a range of scales, from local, through to regional, national, continental, and ultimately to the global scale. Having access to the entire Landsat archive, spanning five decades, and the frequent revisits provided by the current Landsat-8 and -9 combination provides unprecedented streams of evidence from which to inform policy, with relevance to concerns related to land use change, biodiversity, and protected areas (e.g., Bolton et al., 2019; Nagendra et al., 2013). Globally-consistent data are a prerequisite to forming, informing, and complying with policies that operate worldwide. Nations and international agencies require confidence that data streams for monitoring, reporting, and verification can be relied upon into the future. National uptake and agreement to participate in international programs is aided by the forward-going commitments by the USGS for free and open access data and continuity of observations. The Rio Conventions indicated the importance of systematic observations (CBD, 1992), as have the Essential Climate Variables of the United Nations Framework Convention on Climate Change (UNFCCC; Dolman et al., 2016; GCOS, 2016), Essential Biodiversity Variables for the Convention on Biological Diversity (Pettorelli et al., 2016) and Progress Indicators for the United Nations Convention on Combating Desertification (Sommer et al., 2011). Success in addressing Sustainable Development Goals (SDG) targets is also being measured with over 200 assessment indicators (UNESG, 2020). The variables and indicators required for these Multilateral Environmental Agreements have different levels of detail, measurement frequency (e.g., days, years, decades) and geospatial resolution (e.g., m, km, country/region), while some are more qualitative in nature.

Table 2 identifies variables and indicators required by select Multilateral Environmental Agreements where Landsat has already made a significant contribution or where the information derived from Landsat (based upon the level of spatial detail and mappable categories) is

Table 2
Variables/indicators where the spatial and temporal characteristics of Landsat support metric generation. The ability of Landsat to map to categories of importance and interest guides metric definition. Variables and metrics sourced as follows; United Nations Framework Convention on Climate Change (UNFCCC; GCOS, 2016), Convention on Biological Diversity (CBD; Pettorelli et al., 2016), Sustainable Development Goals (SDG; UNESG, 2020).

Variable; Target Metrics
UNFCCC: Glacier area; 15–30-m horizontal / annual end of ablation season
UNFCCC: Glacier elevation change; 30-m horizontal, 1-m vertical / decadal
UNFCCC: Ice velocity; 100-m horizontal / annually
UNFCCC: Area covered by snow; 1-km horizontal /day, 100-m horizontal/day in complex terrain
UNFCCC: Lake area; 20-m horizontal / daily
UNFCCC: Lake color; 300-m horizontal / weekly
UNFCCC: Lake Surface Temperature; 300-m horizontal / weekly
UNFCCC: Land cover classes; 10–30-m horizontal / annually
UNFCCC: Burnt area; 30–250-m horizontal / daily
CBD: Ecosystem structure (including forest cover, land cover); metrics unspecified
CBD: Ecosystem function (including fire disturbance, inundation); metrics unspecified
UNCCD: Trends in land cover, distribution of land cover types; metrics unspecified
UNCCD: Trends in land productivity or functioning of the land, Land productivity dynamics; horizontal unspecified / five yearly
SDG: Target 2.4. By 2030, ensure sustainable food production systems and implement resilient agricultural practices that increase productivity and production, that help maintain ecosystems, that strengthen capacity for adaptation to climate change, extreme weather, drought, flooding and other disasters and that progressively improve land and soil quality. Indicator 2.4.1 Proportion of agricultural area under productive and sustainable agriculture
SDG: Target 3.d. Strengthen the capacity of all countries, in particular developing countries, for early warning, risk reduction and management of national and global health risks. Indicator 3.d.1 International Health Regulations (IHR) capacity and health emergency preparedness
SDG: Target 6.6. By 2020, protect and restore water-related ecosystems, including mountains, forests, wetlands, rivers, aquifers and lakes. Indicator 6.6.1 Change in the extent of water-related ecosystems over time
SDG: Target 9.1. Develop quality, reliable, sustainable and resilient infrastructure, including regional and trans-border infrastructure, to support economic development and human well-being, with a focus on affordable and equitable access for all. Indicator 9.1.1 Proportion of the rural population who live within 2 km of an all-season road
SDG: Target 11.3. By 2030, enhance inclusive and sustainable urbanization and capacity for participatory, integrated and sustainable human settlement planning and management in all countries. Indicator 11.3.1 Ratio of land consumption rate to population growth rate
SDG: Target 15.1. By 2020, ensure the conservation, restoration and sustainable use of terrestrial and inland freshwater ecosystems and their services, in particular forests, wetlands, mountains and drylands, in line with obligations under international agreements. Indicator 15.1.1 Forest area as a proportion of total land area, and 15.1.2 Proportion of important sites for terrestrial and freshwater biodiversity that are covered by protected areas, by ecosystem type
SDG: Target 15.2. By 2020, promote the implementation of sustainable management of all types of forests, halt deforestation, restore degraded forests and substantially increase afforestation and reforestation globally. Indicator 15.2.1 Progress towards sustainable forest management
SDG: Target 15.3 By 2030, combat desertification, restore degraded land and soil, including land affected by desertification, drought and floods, and strive to achieve a land degradation-neutral world. Indicator 15.3.1 Proportion of land that is degraded over total land area
SDG: Target 15.4 By 2030, ensure the conservation of mountain ecosystems, including their biodiversity, in order to enhance their capacity to provide benefits that are essential for sustainable development. Indicator 15.4.2 Mountain Green Cover Index
SDG: Target 15.5 Take urgent and significant action to reduce the degradation of natural habitats, halt the loss of biodiversity and, by 2020, protect and prevent the extinction of threatened species. Indicator 15.5.1 Red List Index

possible. The maturing relationship between the remote sensing and policy communities is exemplified by the evolution of the Hansen et al. (2013) global canopy cover change product to a more holistic land use status and change product (Hansen et al., 2022) and by the adoption of Landsat derived global surface water and wetland extent products and tools as indicators for SDG 6.6.1 (Hakimdavar et al., 2020; Pekel et al., 2016; Weise et al., 2020).

3. Fifty years of Landsat: science and programmatic impact areas

3.1. Agricultural crop mapping and water use

From the advent of Landsat in 1972, a means to map and monitor crops (Kauth and Thomas, 1976) in individual fields and over large regions was newly possible. To demonstrate this, a field campaign known as the Large Area Crop Inventory Experiment (LACIE) was initiated jointly by US Department of Agriculture (USDA), NOAA, and NASA (MacDonald, 1984). LACIE had a domestic aim of estimating planted wheat acreage in the US Great Plains (MacDonald et al., 1975), and also a broader goal to monitor foreign production (MacDonald and Hall, 1980). Follow-on research formed the Agriculture and Resources Inventory Surveys through Aerospace Remote Sensing (AgRISTARS) program which also investigated the collection of corn and soybeans acreage statistics in the US Corn Belt (Caudill and McArdle, 1979; MacDonald, 1984). These pioneering studies also gave rise to corresponding work elsewhere in the world, such as Europe's Agricultural Resources Investigations in Northern Italy and Southern France (AGRESTE) project. Undertaken with NASA, the AGRESTE project used Landsat imagery to inventory European agricultural crops and forests and was the precursor for crop mapping in the context of European agricultural policies that continue today (Chakhar et al., 2020). Early results were mixed given challenges including slow imagery delivery and substantial effort needed to process the data. Despite these limitations, Hall and Badhwar (1987) successfully demonstrated an approach based on the Tasseled Cap transform of multi-date Landsat Multispectral Scanner (MSS) data which enabled the incorporation of model-based, greenness-time trajectories for each crop. The separability and identifiability aspects of the multi-date signature extension approach developed were a valuable precursor of time-series-based analyses to come. Combined multitemporal and multispectral application of Landsat MSS data was also explored by Badhwar (1984), enabling an automated, large-area, multi-year, estimation of corn and soybean crop proportions. Development of improved methods for identifying commodity crops from Landsat imagery continued through the years (Rudorff and Batista, 1991; Thenkabail et al., 1994). The finer 30-m spatial resolution offered by Landsat-4 and -5 Thematic Mapper (TM) launched in 1982 and 1984 led to improved agricultural mapping and with Landsat time series provided tracking of crop condition and yield through the growing season (Carfagna and Gallego, 2006; Doraiswamy et al., 2004). During this time there was also a shift from the research being primarily housed within the US Federal Government to a broader usage within universities and international institutions.

More powerful computing systems with greater data-handling capabilities, in conjunction with machine learning classification methods, eventually allowed for the first conterminous US crop area map via the National Land Cover Database (Vogelmann et al., 2001). The US Department of Agriculture (USDA) National Agricultural Statistics Service (NASS) began using Landsat, supplemented with other medium resolution satellite imagery, and extensive agricultural ground reference data, to derive the 30-m Cropland Data Layer (CDL; Boryan et al., 2011; Johnson and Mueller, 2010). The CDL defines annually, with a lag of one year, approximately 110 land cover and crop type classes and is used to provide acreage estimates, corroborate within season on-the-ground planted area survey information, and to inform coarser resolution depictions of crop specific condition and yield assessments (Johnson, 2019). The shift in data policy allowing for free Landsat imagery expanded research dedicated to crop monitoring, accelerating capabilities for regional to global cropland mapping outside of federal agencies (Fritz et al., 2015; King et al., 2017; Pérez-Hoyos et al., 2017; Song et al., 2017). The ability to generate robust crop maps over large areas has allowed the institutionalization of such maps.

Landsat imagery has underpinned improved understanding of regional cropping systems, beyond the generation of agricultural census

information. For example, Landsat data have enabled the mapping of field sizes (Pitts and Badhwar, 1980; Yan and Roy, 2016), tracking of crop progress (Gao et al., 2017), mapping of crop residues and tillage practices (Beeson et al., 2020; Zheng et al., 2012), as well as providing a means to map crops retrospectively (Johnson, 2019). Biophysical measurements such as estimation of gross primary production (Gitelson et al., 2012) and plant water content (Anderson et al., 2004; Jackson et al., 2004) have also been performed.

Landsat also has a rich history in quantifying crop water use, availability, and stress impacts on yield through evapotranspiration modeling and critically rely on thermal observations (Anderson et al., 2012). Widespread irrigation mapping at a Landsat scale has only been undertaken recently (Chen et al., 2018b; Deines et al., 2017) and the availability of the Landsat archive on Google Earth Engine has enabled routine generation of field-scale evapotranspiration products in support of water management applications (Senay et al., 2022). An example of such products are those developed for the western US under the OpenET project, a collaborative effort involving federal, academic and non-profit partners working closely with stakeholders to develop a Landsat-based water use information system that can be efficiently and effectively integrated with existing tools for irrigation scheduling, water allocation and conservation, water trade negotiations, sustainable groundwater management planning, and ecosystem assessment among others (Melton et al., 2021). The Google Earth Engine based platform (https://openetdata.org/) enables open and easy access for all parties to historic and real-time evapotranspiration (ET) data, incorporation of latest science, as well as transparency and community review of dataset robustness. The web-based interface was designed for visual data exploration and extraction (Fig. 5), while the OpenET Application Programming Interface (API) allows direct data queries and ingestion into existing operations and decision-support systems. OpenET is a prime example of the transformational impact that the free Landsat archive is having, in concert with expanding cloud computing power, on our ability to better steward Earth's resources.

Ultimately, the early use of Landsat for addressing agricultural questions provided unique and otherwise unavailable information and also pointed to the utility of satellite remote sensing for both domestic purposes in the US and at the global scale. Further, non-agricultural sectors were able to point to the demonstrated utility and to identify opportunities for their particular sector. This provided a broadening of the user base and Landsat program supporters across US government agencies (Mack, 1990).

3.2. Climate change drivers and impacts

Climate is generally considered as the prevailing weather over a 30-year period, which is longer than any single satellite sensor mission. The advent of collection-based reprocessing nominally provides consistent sensor measurements among the Landsat missions back to 1972 with a longevity that is unique for detecting and determining the effects of climate change. However, successive Landsat missions were characterized by improvements in spatial, spectral, radiometric and/or temporal resolutions and so intercomparison of Landsat imagery from different sensors may need to be carefully considered. The most recent Collection 2 reprocessing does not normalise for all differences among Landsat sensors (Section 2.1). For example, the Landsat MSS on Landsats 1–5 acquired 6-bit radiometric resolution images with 79-m pixels based on a 57 × 79 m ground sampling distance in green, red, and two near-infrared bands (Goward et al., 2017). The Landsat MSS geolocation is less reliable than for more recent Landsat sensors (Yan and Roy, 2021) and currently there is no broadly applicable MSS cloud mask or atmospheric correction algorithm due to the low MSS spectral resolution. Another example, is the extraordinary 27-year mission life of Landsat-5 that provided the longest operating Earth remote sensing satellite

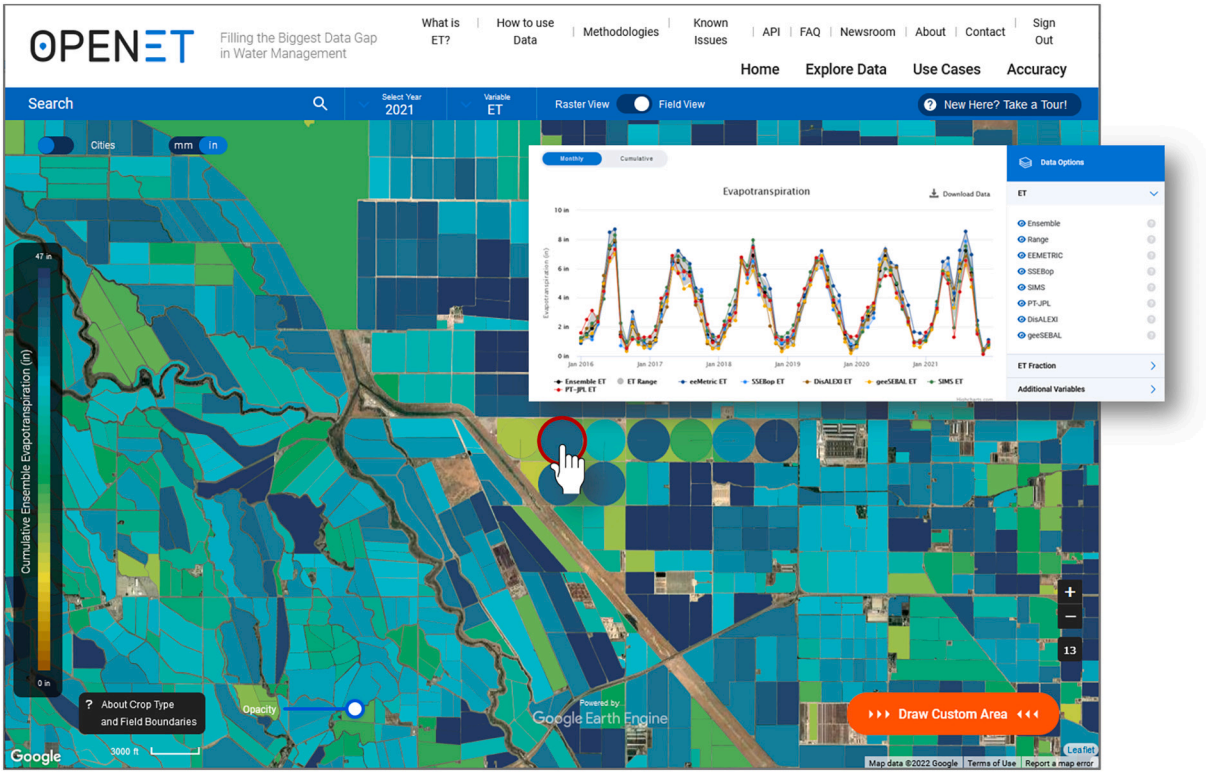

Fig. 5. The OpenET data explore interface on Google Earth Engine enables free and open access to Landsat-derived 30-m evapotranspiration data created with an ensemble of modeling systems. This example shows an extraction of multi-model monthly evapotranspiration time series over a center-pivot irrigated field (denoted by pointer and red circle) in the Central Valley of California, as well as an ensemble average, noting that data can also be viewed in gridded form (see: https://openetdata.org/). (For interpretation of the references to colour in this figure legend, the reader is referred to the web version of this article.)

mission in history. The Landsat-5 satellite had significant orbital drifts, particularly during the commercial Landsat era, with changes in the overpass time of nearly 1 h and changes in the observed solar zenith angle >10°, resulting in periods where changes in land surface reflectance may be due largely to orbital drift (Zhang and Roy, 2016). These and other issues are subject to ongoing research (Braaten et al., 2015; Qiu et al., 2021) aimed to ensure the quality and integrity of historic observations with the more robust observations from current Landsat missions. Due to the subtlety of some climate change effects of interest, it is important to be aware of systematic or measurement issues possibly impacting analyses. Given the length of the Landsat record, and the important and dynamic era in human history represented, the climate change phenomena evaluated require circumspect analysis, granting that trends may also be informed or corroborated by AVHRR or MODIS (e.g. Che et al., 2021).

Despite the above caveats, for the purposes of understanding climate change drivers and impacts Landsat provides an extremely valuable record of information. As landscape, hydrologic, and cryospheric features have evolved due to warming or changing rainfall (or snowfall), Landsat has provided the decadal perspective necessary to both measure the change and to present it, vividly and understandably, to the public. The geographic coverage and frequency of Landsat acquisitions have varied over the last 50 years. Locations outside of the US or not in proximity to an International Cooperator receiving station were often not acquired in the initial decades of the program. It was not until the introduction of a long-term acquisition plan (Arvidson et al., 2001) that routine global observations were secured after the launch of Landsat-7 in 1999 (Wulder et al., 2016). Consequently, in some terrestrial regions, the temporal record may be sparse (e.g. Saarinen et al., 2018). Given this context, major climate related applications of Landsat are associated with forest change characterization, desertification, changes in surface water extent, as well as changes in the expanse and surface albedo of seasonal snow, glaciers, and the polar ice sheets.

The ability of Landsat to track environmental change and climate change impacts was recognized early in the mission series (Goward and Williams, 1997; Goward, 1989). Among the first climate-related applications were mapping of forest succession and burned areas with a view towards climate trends and carbon sequestration (Foody et al., 1996; Hall et al., 1991), and lake extent changes and desertification (Schneider et al., 1985; Trefois, 1995). Landsat also saw early use tracking glacier and ice sheet areas, detecting changes in their extent over time in order to identify regional climate trends (Jacobs et al., 1997; Li et al., 1998). Basic mapping of the polar regions—areas that are fundamentally susceptible to change driven by climate or ocean conditions—was also an early target of research (Williams et al., 1982, 1995). Since then, most assessments of large-scale, regional-to-continental climate change impacts have employed the temporal perspective and spatial resolution that the Landsat sensor series offers. The observed warming in northern tundra and boreal forest regions was anticipated to cause observable changes in those biomes (Beamish et al., 2020). An example of such studies includes research illustrating greening of high-latitude shrub and grassland areas and browning of regions that are drying as a result of earlier snowmelt and permafrost lake drainage, induced by increased summer warmth in large areas of Alaska and Canada (Ju and Masek, 2016). Siberian tundra areas showed a similar impact in the 1984–2012 Landsat record with high percentages of tundra and alder shrublands showing greening (Frost et al., 2014).

The extended Landsat record has also provided a unique record of long-term subtle forest changes. Cohen et al. (2016) provide a comprehensive study of forest changes in the coterminous US based on a Landsat analysis spanning 1985 through 2012. The subtle change patterns identified from the Landsat record reveal the processes causing changes and related physical drivers. Many of these, such as fire and insect damage, are directly attributable to climate change, particularly in the mountain west and lowland west states under investigation. Analysis of Landsat time series enables the generation and characterization of trends, offering insights on drivers of change, such as vegetation stress or insects, when land cover does not change but land condition does (Coops et al., 2020).

Surface water extent (exclusive of the oceans) has also been identified as a sensitive indicator of climate change, dependent on rainfall and snowfall, evaporation rates, and the status of surrounding vegetation. Building upon isolated lake changes typical of earlier assessments, with hard-to-attribute causes (Buma et al., 2018; Ouma and Tateishi, 2006), more comprehensive studies aimed, first, to use the global coverage of Landsat to map surface water extent (Yamazaki et al., 2015) and then its extended temporal record to document changes and begin to attribute them (Pekel et al., 2016).

Perhaps the most dramatic shifts due to climate change have occurred in the cryosphere: the snow, lake- and sea-ice, and continental ice sheet components of the Earth system. As a result of the readily observable physical aspects of snow and ice landscapes, i.e., their unique high albedo, and their spectral and textural characteristics, the Landsat archive has played a major role in documenting major changes over the past five decades. Snow cover globally is dominated by the Northern Hemisphere trends, which show decline in spring, but may be increasing in fall, over the past 50 years (Ballinger et al., 2018; Connolly et al., 2019). However, the scale of processing required to quantitatively assess snow cover (which changes rapidly and has a significant mixed-pixel component; Dozier and Marks, 1987; Rosenthal and Dozier, 1996) has to date, limited Landsat's contribution to determining long-term, large-region trends. Nonetheless, significant decreases in persistent ice and snow cover have been quantified over globally disparate regions using the Landsat temporal record and spectral indices (Bevington and Menounos, 2022; X. Chen et al., 2018a; Park et al., 2016; Selkowitz and Forster, 2016). Another consequence of reduced precipitation or earlier run-off in glaciated regions is the increasing number of dust-depositing events on mountain snow. These have been shown to significantly impact runoff timing and volume (Painter et al., 2018). More recently, detailed Landsat-derived albedos associated with extreme warming events on the Greenland Ice Sheet have been captured (Elmes et al., 2021), providing a better understanding of the variations in the surface energy budget and radiative forcing occurring in this region.

Sea ice decline over the past 50 years has been monitored mostly by passive microwave satellites, but Landsat has played an important role in characterizing sea ice surface types at a finer spatial resolution than the multi-kilometer spatial resolution typical of passive microwave sensors (Comiso and Steffen, 2001; Steffen and Heinrichs, 1994) and defining surface mapping parameters for the complex sea ice surface during the melt season (Markus et al., 2003). More recently, Landsat has been used in intercomparison and calibration of multiple mapping tools for sea ice concentration (Kern et al., 2022). The use of Landsat's thermal mapping capability has also been exploited for polar winter mapping of sea ice leads (Hoffman et al., 2019). Furthermore, the Landsat satellite series has played a major role in research on climate-related changes on glaciers and the major ice sheets. The five-decade record has spanned the dramatic retreat of several of the Earth's mountain glacier regions, in many cases detailing their complete disappearance (e.g., Seehaus et al., 2019). The advent of tools for tracking surface meltwater on the ice sheets (Kingslake et al., 2017; Moussavi et al., 2020) and ice flow speed (Fahnestock et al., 2016; Scambos et al., 1992), coupled with the large increase in global and polar acquisitions, has transformed our ability to monitor ice sheet conditions and ice sheet flux to the ocean on an annual and even seasonal basis (Gardner et al., 2018; Joughin et al., 2018), as shown for Antarctica (Fig. 6).

3.3. Ecosystem and land cover monitoring

Current understanding of the status and dynamics of global ecosystems is widely informed by Landsat data, with insights of scientific, management, and policy relevance. Long-term ecological change has been observed and documented using Landsat, the implications of which

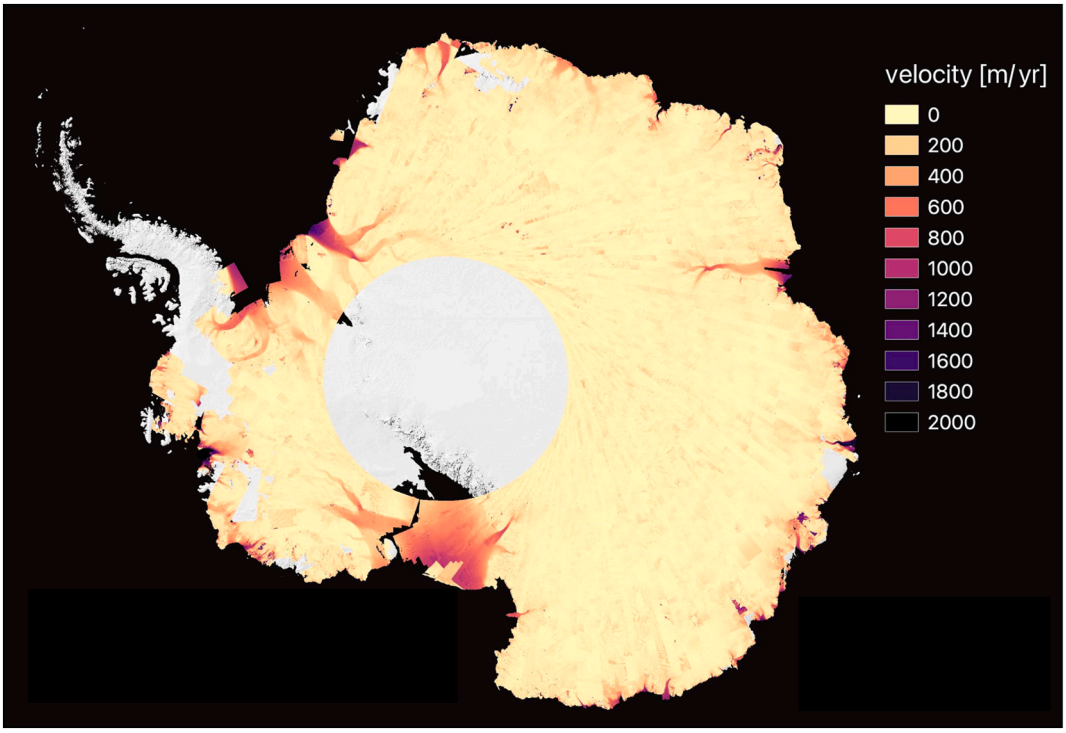

Fig. 6. Antarctic surface velocities determined by measuring small displacements in thousands of pairs of repeat Landsat-9 images using autoRIFT software (Gardner et al., 2018) and provided by the NASA MEaSUREs ITS_LIVE project (Gardner et al., 2022) that provides low latency, global glacier flow and elevation change datasets. Landsat-9 imagery acquired between Oct. 31, 2021 and Feb. 14, 2022, and reflect some preliminary issues with geolocation of the scenes (speckled appearance).

are regional, national, and international. Landsat data and analytical methods have led to and continue to inform polices aimed at improved natural resource management. Terrestrial ecosystems can be characterized by land cover, changes in land cover, and the structure of the vegetation present. Landsat enables the mapping of all these characteristics, as well as monitoring of these elements over time. Three years prior to the launch of the first Landsat satellite in 1972, Odum (1969) summarized a prevailing view of ecology when he described community development as a reasonably predictable and directional progression toward an expected outcome. More than any other tool, Landsat has forced us to confront ecological change that is less predictable and more pervasive than we previously imagined (Kennedy et al., 2014). From the program's inception, Landsat demonstrated the capacity to map change in forest ecosystems (Williams and Miller, 1979). Hansen et al. (2013) applied that capacity globally, creating our first consistent look at forest dynamics (forest loss and bare ground gain) across the planet for a decadal period. Even in apparently stable forest ecosystems, researchers have used Landsat to uncover ubiquitous slow or subtle disturbance processes (Bullock et al., 2020a; Cohen et al., 2016; Coops et al., 2020; Vogelmann et al., 2015). Further, forest changes due to urbanization and agricultural expansion, which are more permanent in nature, can be separated from changes that are not indicative of a land use change per se, but rather a temporary change in land cover such as wildfire or harvesting (Hermosilla et al., 2015a; Kennedy et al., 2015). Time series of Landsat data also offer a means to capture and quantify the return of vegetation at these sites following disturbances, often described as forest recovery (Kennedy et al., 2010, 2012; White et al., 2017, 2022).

Across a variety of biomes, Landsat is increasingly used as a tool for continuous instead of periodic monitoring, accounting for changes of all kinds beyond discrete disturbances (Woodcock et al., 2020). For example, while Landsat provided stunning detail of the effects of the Mt. St. Helens volcanic eruption in 1980 (Bohn and Bly, 1981), an even bigger contribution may be direct observation of subsequent forest formation processes in the absence of nearby seed sources or organic soil (Lawrence and Ripple, 2000) (Fig. 7). Landsat's evapotranspiration mapping capabilities have been used to link drought-related stress to tree mortality at time lags of a year or more (Yang et al., 2021).

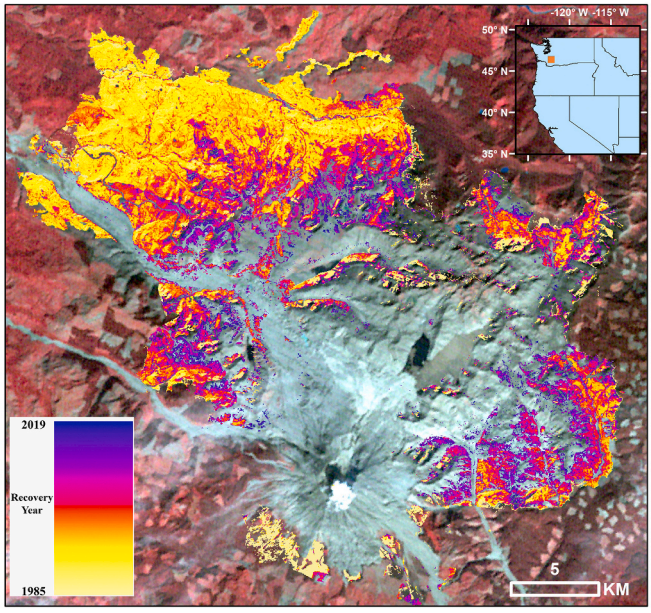

Fig. 7. Landsat observed the eruption of Mount St. Helens (May 18, 1980) and has enabled tracking steady recovery of nearby forests in the years since. Dates represent the first year of Landsat-modeled canopy cover of over 50% (after Healey et al., 2006). False color composition (bands: near infrared, red, green) used for the background Landsat image. (For interpretation of the references to colour in this figure legend, the reader is referred to the web version of this article.)

Supported by the opening of the archive and expanding computing resources, change detection methods have evolved from two-date comparisons (Coppin et al., 2004) to include time series analyses (Zhu, 2017) that uses annual composite imagery (Hermosilla et al., 2015b; Huang et al., 2010; Kennedy et al., 2010) and all available imagery (Zhu and Woodcock, 2014) as well as ensembles of such algorithms (Healey et al., 2018).

Land cover mapping, an application for which Landsat's spectral and spatial properties are particularly well suited (Hansen and Loveland, 2012), has gradually evolved to explicitly account for change in land cover class (Brown et al., 2020; Byrne et al., 1980; Hermosilla et al., 2022; Homer et al., 2015; Pickens et al., 2020). This development enables the explicit inclusion of disturbance and knowledge of successional processes into classification models, thus providing a richer and more dynamic picture of Earth's ecosystems (Wulder et al., 2018). The ability to capture (when and where) and identify changes (what) enables insights on the drivers and implications of remote sensing derived changes (Fig. 8). Land cover can be interpreted as a function of time before and after a given disturbance event. In Fig. 8, the maturing of forests demonstrated by a reduction in herbaceous and shrubs classes prior to harvesting of trees is mirrored after disturbance. The removal of trees can be seen, with a temporal dominance of herb and shrubs as ecological processes are followed towards a return to tree cover (Hermosilla et al., 2018). In Canada, the highest detailed and most spatially comprehensive maps of forest harvesting are those derived from Landsat (Hermosilla et al., 2016).

The use of Landsat as a monitoring tool has often involved integration with data from other sensors. MODIS' daily acquisition and similar passive optical measurements have offered the opportunity to enhance Landsat's surface reflectance signal for applications, including creating temporally-interpolated imagery (Hilker et al., 2009); improving Landsat fire history maps (Boschetti et al., 2015), and monitoring daily crop phenology (Gao et al., 2017) and surface albedo products (Liu et al., 2017; Wang et al., 2017). Landsat has also been used to aid in spatial extrapolation of sampled forest vertical structure information, typically from lidar, over space (Healey et al., 2020; Potapov et al., 2021) and time (Matasci et al., 2018). Landsat provides spectral information to act as predictor layers in modeling forest structure in a spatially exhaustive fashion. Calibrated reflectance, as a physical value, allows for model portability over time, enabling the modeled generation of a time series of forest structure from Landsat data (Matasci et al., 2018; Song et al., 2001). Spatially-exhaustive maps of forest structure (e.g., biomass, volume, height, canopy cover) significantly expand the ecosystem monitoring questions that Landsat can address. Similarly as Landsat fundamentally altered our understanding of ecological complexity in its first fifty years (Kennedy et al., 2014), improved data systems and algorithms are likely to catalyze further discoveries and spur operational monitoring programs.

3.4. Anthropogenic impacts

When the first Landsat was launched in 1972, global population was approximately 3.8 billion people. Since then Earth's population has more than doubled (OECD, 2020). Concurrently, the footprint of

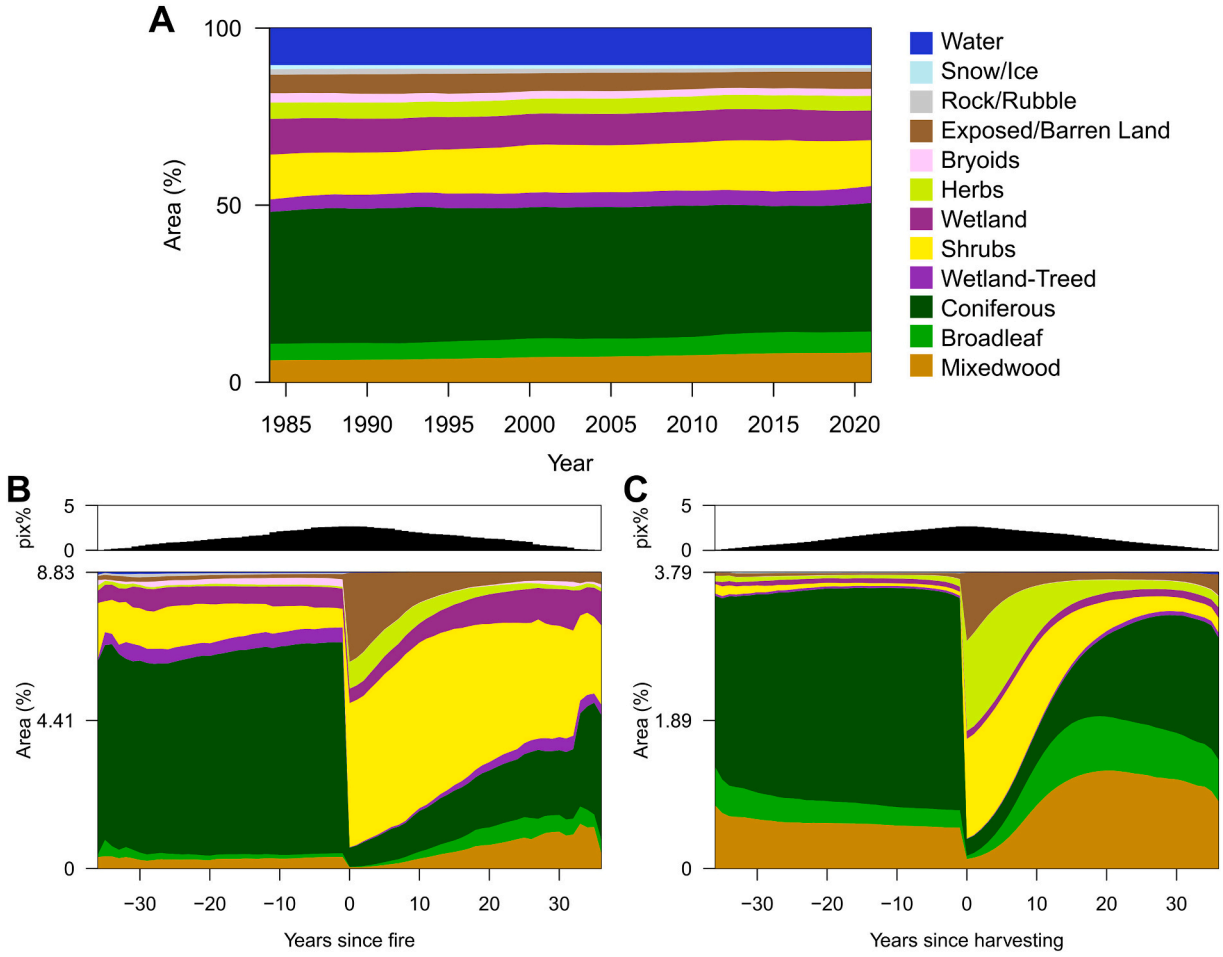

Fig. 8. Class proportions by year for Canada's forest dominated ecosystems, representing 650 million hectares and 38 years of land cover dynamics derived from Landsat data (A). Using independently-detected and labeled forest disturbances, the land cover characteristics can be understood as a function of time prior to and following disturbance events by type: wildfire (B) and harvesting (C) (updated after Hermosilla et al., 2018).

humankind on Earth has grown, particularly with respect to urban development, agricultural land expansion, and the increasing extraction of natural resources, which have contributed to climate change, land degradation, and biodiversity loss. Indeed, over the last 10,000 years, human activity is attributed to modifying over 70% of Earth's land surface (Ellis, 2021). The Landsat satellite record provides a critical resource for understanding recent anthropogenic impacts (Pesaresi et al., 2016) and has resulted in unique insights into the socioeconomic causes of these changes and their consequences for the environment, ecosystem services, and hence humankind. For example, Landsat data have documented a more than doubling of global built-up area from 379,552 km^2 in 1975 to 789,385 km^2 in 2014 (Corbane et al., 2019), and mapped global cropland areas (19.3 million km^2 in 2010) and cropland area change (increased by ~2% from 2000 to 2010) (Hu et al., 2020).

To understand human impacts to our global ecosystem, the first step is to map land use and land use change (Winkler et al., 2021). Land cover is a representation of the geo-biophysical properties associated with the land surface, whereas land use reflects economic activities or the functional use of the land (Comber et al., 2008; Lambin et al., 2001; Townshend, 1992). Compared to land cover mapping, it is much more challenging to map land use from Landsat data. Land use represents a socio-economic criterion and disentangling the land use dimension from satellite data requires knowledge of human agency and intent (Kuemmerle et al., 2013). In particular, satellite observations of reflected and/or emitted radiation do not necessarily contain the information needed to separate different categories of land use (e.g. both a park and a managed forest are different land uses of treed land cover). Nevertheless, Landsat data are still considered the gold standard for mapping land use and land use changes because of the medium spatial resolution, multispectral bands, and long temporal record (Gordon, 1980; Seto et al., 2002; Sieber et al., 2013; Welch et al., 1975).

The launch of Landsat-1 enabled—for the first time—regular and continuous global urban monitoring using repeat observations from satellite remote sensing (Haack et al., 1987). The addition of an operational thermal band and 30-m spatial resolution shortwave bands with Landsat-4 greatly advanced urban remote sensing and allowed analyses of urban heat islands (Aniello et al., 1995) and the mapping urban areas at higher spatial resolution at regional to global scales (Gong et al., 2020; Liu et al., 2018; Xian et al., 2009). Currently, with the availability of dense Landsat time series and other urban-related open data (e.g., Hu et al., 2016), new research directions such as high-frequency analysis of urban disturbance, urban heterogeneity, and urban form are now possible (Zhu et al., 2019b).

Advances have been made in applying Landsat in land use mapping, including the characterization of croplands, built-up areas, and deforestation (Corbane et al., 2019; Hansen et al., 2022; Lindquist and D'Annunzio, 2016; Potapov et al., 2022; Zalles et al., 2021; Zhu et al., 2019b). Natural capital in the form of forests, grasslands, wetlands, and other land cover categories absent of land use account for key ecosystem functions, including climate regulation, biodiversity habitat, water quality, and other services. The conversion of natural lands into land use systems impacts the provisioning of these services. For example, 23% of anthropogenic forcing of global climate warming is attributable to land use change (IPCC, 2019). Monitoring land use expansion is a critical measure in assessing the sustainability of natural systems. Such human-footprint analysis approaches rely principally on land use layers that depict agriculture, settlements, and built infrastructure (Sanderson et al., 2002; Venter et al., 2016), with many such layers employing coarse spatial resolution land cover / land use layers. Specific high conservation value land cover categories, such as the forests of the humid tropics can be mapped directly and detected loss quantified over time (Turubanova et al., 2018). Global Landsat characterizations of land cover and land use are much more appropriate for such assessments given that land use extent and change is often a fine-scale phenomenon better depicted at medium spatial resolutions. New assessments of land use in studying human impact on natural lands are advancing this study area. Fig. 9 shows a subset of a global land use and dispersion analysis derived from Landsat (Hansen et al., 2022).

Intensification of land use is implicit in mapping land use types. For example, impervious surfaces, such as roads and rooftops, depict human-built surfaces and represent arguably the most impactful conversion of land cover (Yuan and Bauer, 2007). Croplands are more easily characterized when taking the form of intensive, high input, large field size commodity crop production; however, by comparison, low-intensity shifting-cultivation land uses are more challenging to characterize (Schneibel et al., 2017). Many land use disturbances represent degradation, or the partial modification of natural land cover, for example the selective logging of rainforests (Bullock et al., 2020b). Such disturbances often do not result in a discernable land use change, but still represent an important impact on natural land covers. For example, a long-term Landsat study estimated that from 1985 to 2018 in South America, 55 Mha of natural land cover were disturbed by human activities not associated with a clearly identifiable land use (Zalles et al., 2021). Studies using Landsat have demonstrated a capability to track humid tropical forest degradation, improving forest carbon stock loss and resulting committed emissions (Tang et al., 2020).

When humans use land, they affect species' habitat, with habitat loss as a major cause of biodiversity loss (Sala et al., 2000). Landsat imagery captures where species' habitats occur (Scott et al., 1993), providing required data to species distribution models that often underlie biodiversity monitoring (Duro et al., 2007; He et al., 2015; Turner et al., 2003, 2015). For example, Landsat data highlight the importance of vegetation productivity (Duro et al., 2014; St-Louis et al., 2009), horizontal vegetation structure (Farwell et al., 2021), and winter habitat conditions (Homer et al., 1993; Rickbeil et al., 2020) for biodiversity patterns. Landsat-1—3 MSS and Landsat-4 and -5 TM data have been used to highlight long-term locations with significant habitat loss (Hansen et al., 2001; Leimgruber et al., 2005). The improved 30-m resolution provided by the Landsat TM first launched in 1982 and present on successor Landsat sensors has improved the ability to identify the impacts of habitat fragmentation (Echeverria et al., 2006; Skole and Tucker, 1993) and the ecological benefits of landscape connectivity (Bleyhl et al., 2017). Landsat time series analyses have enabled advances in the characterization of forest fragmentation trends and the return of vegetation to resemble pre-disturbance conditions (Hermosilla et al., 2019), highlighting the role of fragmentation as a process and not just a state. Landsat data have also uncovered when parks are not serving their intended protective function (Liu et al., 2001) and when parks are isolated islands in areas of intensive human land use (DeFries et al., 2005; Nagendra et al., 2013). Landsat time series also enable retrospective assessments on the protective function of parks and protected areas, with research demonstrating level of protection varying by proximity to human populations and disturbance type (e.g., wildfire, harvesting; Bolton et al., 2019). Undoubtedly, one of Landsat's most important legacies to date is the provision of an objective baseline for future monitoring of terrestrial ecosystems that is not subject to changing perceptions of naturalness or management priorities over time (White et al., 2019). The quantification of these dynamics is critical as land use extensification and intensification are key concerns in balancing of economic development with environmental sustainability.

4. Outlook: Landsat continuity

4.1. Landsat-9: Early insights

NASA successfully launched Landsat-9 from Vandenburg Space Force Base, California on September 27, 2021, and its on-orbit commissioning phase was completed with the start of operations in January 2022. The Landsat-9 observatory carries both the Operational Land Imager 2 (OLI-2) and the Thermal Infrared Sensor 2 (TIRS-2) that mirrors its sister satellite, Landsat-8, to continue eight-day multispectral imaging of all global landmasses and near-shore coastal regions (Masek

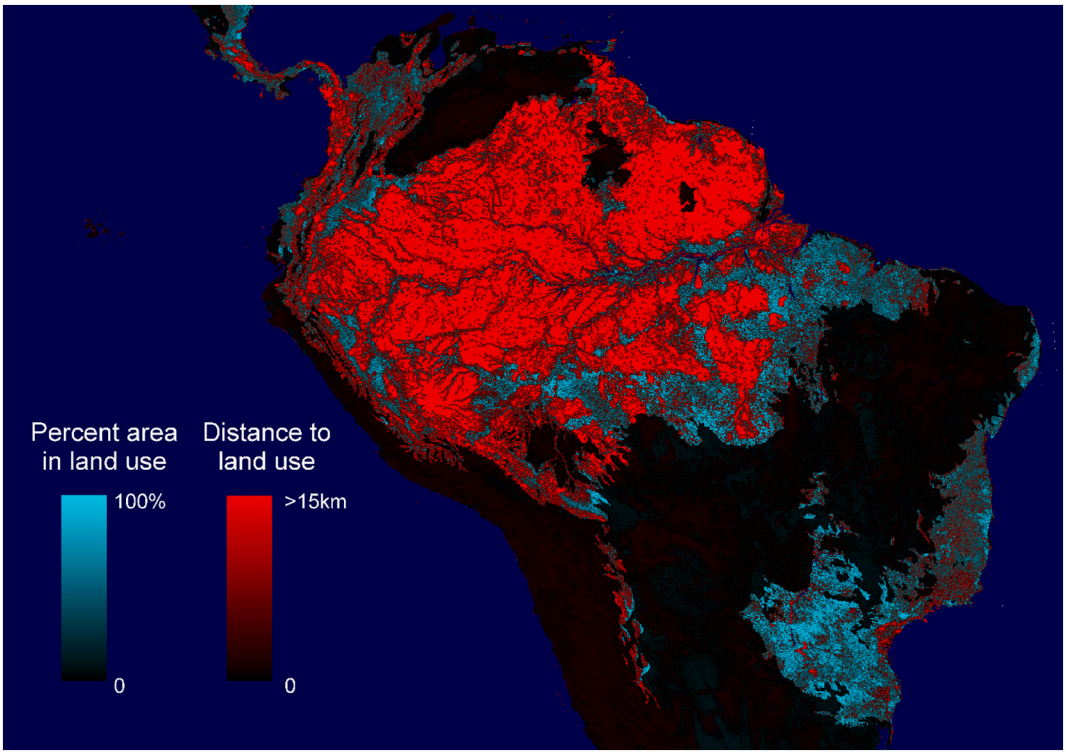

Fig. 9. Area of land use and distance to land use for the humid tropical forests of South America, where intensive land uses and natural land covers were derived from Landsat data (after Hansen et al., 2022). Red indicates extant humid tropical forest absent of land use and located more than 15 km from land use. (For interpretation of the references to colour in this figure legend, the reader is referred to the web version of this article.)

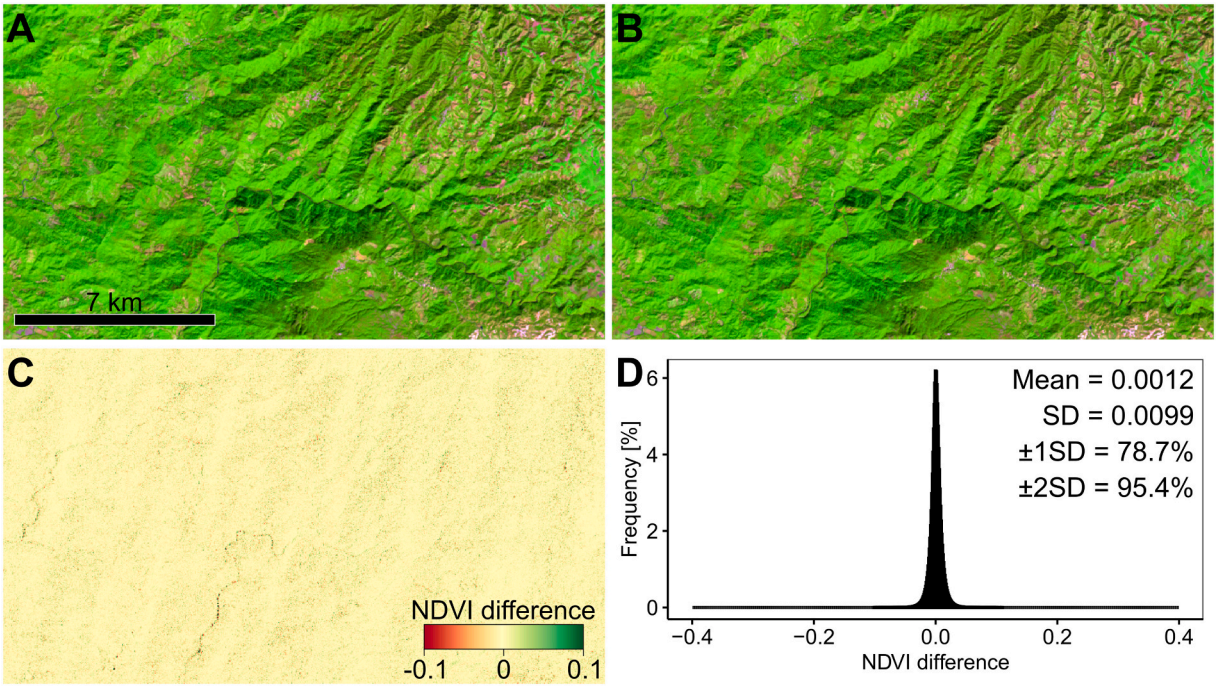

Fig. 10. Underfly comparison showing a detail from scene with path/row: 030/045. Geographic position: lat/lon: 21.33°N/105.042°W. (A) Landsat-8 and (B) Landsat-9 images in false color composition (short-wave infrared 1, near infrared, red), (C) Normalized differenced vegetation index (NDVI) differences, and (D) histogram (bin size = 0.001) and statistics of NDVI differences. SD: Standard deviation; ±1SD and ± 2SD: percentage of observations falling within ±1 and ± 2 standard deviations, respectively. Note that values above/below the upper/lower limits on panel C are truncated for purposes of graphical representation. (For interpretation of the references to colour in this figure legend, the reader is referred to the web version of this article.)

et al., 2020). Landsat-9 has the privilege of carrying the historical Landsat record on through its 50-year anniversary as the latest Landsat observatory and will continue Landsat's long term data continuity into the next decade. Landsat-9 has several notable improvements over Landsat-8. Notably, the TIRS-2 was upgraded to a fully redundant (Class B) instrument, and the OLI-2 was subjected to more comprehensive pre-launch instrument characterization and calibration using the Goddard Laser for Absolute Measurement of Radiance (GLAMR) (McCorkel et al., 2019). In addition, the Landsat-9 OLI-2 provides improved 14-bit radiometric resolution that will permit improved measurement of subtle variability in surface conditions and is expected to improve data usability over visibly dark Earth surface targets such as dense forests and waterbodies, and bright surfaces such as snow and ice.

Shortly after the start of operations, the USGS released Landsat-9 science data products on February 10, 2022. The available Landsat-9 Collection 2 data products include both scene-based Level-1 calibrated digital counts at TOA, Level-2 atmospherically corrected surface reflectance and surface temperature geophysical measures and ARD for the continental US, Alaska, and Hawaii. These Landsat-9 data products are available for download through the USGS Earth Explorer, EROS Machine-to-Machine (M2M) API, and also directly through the USGS Landsat virtual cloud via the Amazon Web Services (AWS) US West Simple Storage Services (S3) bucket. During the Landsat-9 commissioning phase, an underfly of Landsat-8 was conducted to enable an assessment of Landsat-9's initial geometric and radiometric calibration and measurement performance compared to Landsat-8 (Markham et al., 2021), as illustrated in Fig. 10. The narrow distribution and the near-zero average of the spectral differences between sensors are indicative of the strong spectral agreement of Landsat-8 and -9, as confirmed by Gross et al. (2022). Based on this assessment and unique underfly dataset, Landsat-9 was cross calibrated to Landsat-8 to minimize subtle differences in their TOA observations, thereby maximizing congruousness in cross-sensor, merged downstream products, where Landsat-8 continues to serve as the absolute calibration reference for Landsat Collection 2 product generation. Thus, Landsat data users should have high confidence that Landsat-9 image data have been integrated into Landsat's 50-year data archive to facilitate unbroken data continuity and seamless open science applications.

4.2. Landsat-Next: Continuity plus

The Landsat-9 follow-on mission, currently called Landsat Next, is under formulation with a launch date scheduled for the end of this decade. Landsat Next is considered the cornerstone mission of the Sustainable Land Imaging (SLI) program, a joint NASA and Department of Interior USGS program designed around ensuring US acquired terrestrial land imaging data through the 2030s that is compatible with the long-term Landsat data record (National Research Council, 2013). Over the past several years, NASA and USGS have broadly canvased the remote sensing user community (Wu et al., 2019), the USGS-NASA Landsat Science Team, and US Federal agencies on future Landsat measurement needs as well as proposed Landsat Next science mission requirements. Currently, NASA and USGS envision the Landsat Next mission concept to include a combined 21 visible-to-shortwave infrared and five thermal infrared bands with multiple satellites in orbit together to improve revisit frequency. Higher spatial resolution is being proposed to facilitate greater international Earth observation synergy and enabling monitoring of smaller land parcels worldwide. The configuration of visible-to-shortwave infrared and thermal infrared spectral bands are designed to ensure historical spectral continuity with prior Landsat sensors, estimate instantaneous atmospheric aerosols and water vapor content, provide improved cloud masking, complement current and future Sentinel-2 spectral bands, and enable emerging science applications. New science applications include enhanced monitoring of rivers, lakes, water supplies, and coastal estuaries, measurement of vegetation canopy chlorophyll, snow hydrology, and monitoring of agricultural crop residue and soil properties that require narrow, targeted spectral bands to retrieve physical, biological, and chemical information content. Landsat Next is expected to operate with its counterpart Landsat-9 through the 2030s.

5. Conclusions

As highlighted herein, the scientific and programmatic contributions provided by the past 50 years of the Landsat program are many and varied. These contributions range from ground-breaking changes for the free distribution of medium resolution data via the internet, innovations in data management, medium resolution reprocessing, and provision of robustly calibrated science-grade data, to scientific advances in characterizing terrestrial ecosystems, the processes that shape them, and the rate and magnitude of changes these ecosystems are experiencing. Landsat data have documented decades of anthropogenic activity on the Earth's surface, enabling the quantification of impacts, while also providing the necessary information to understand long-term consequences and enhance stewardship.

Global change science requires long-term, consistent imagery with community endorsed processing and known provenance. Land management applications require consistent baselines, against which changes and trends can be measured. Commercial EO satellite constellations benefit from reliable benchmarks from which to calibrate and geolocate their imagery. Free and open access data are enabling terrestrial environmental monitoring in support of national programs as well as monitoring, reporting, and verification activities linked to multilateral agreements. Community endorsed algorithms and derived products—both subject to scientific scrutiny—are key. Broad access to Landsat data has allowed insights to be gained through a preponderance of evidence from differing perspectives that are no longer limited to singular analyses or outcomes.

Historically, remote sensing scientists would lament about what we did not have and what we could do *if only*. That *if only* was always a future EO system to be built and launched at some unknown date. That is no longer the case. Space agencies have delivered. In many ways, the future is now. There are now commitments to EO satellite launches in a systematic and integrated fashion, exemplified by the NASA-USGS Landsat program and the Sentinel-2 satellites of the European Union's Copernicus program. Both programs have complementary EO satellites, with a long-term operational vision, and decadal funding.

While the focus herein has been on Landsat—a single EO program—as a community, we now have access to complementary programs and observations. Given the open-access imagery from Landsat and Sentinel-2, it is now possible to produce global information products and services, which are needed for management of terrestrial resources, as well as to document and understand change at scales of human influence. Combined these sensors have a 50-year heritage, with Landsat acting as a historic archive for Sentinel-2. The institutional efforts behind ensuring the interoperability of Landsat and Sentinel-2 provide a model for future collaboration and cooperation. Undertaking pre- and post-launch cross-calibration activities adds value to both programs and provides an effective increase in the temporal revisit at medium spatial resolution, to a global mean of 2.3 revisit opportunities per week when including Landsat-8 and-9, Sentinel-2A and -2B, enhancing science and applications activities. Data from both programs are geolocated, cross-calibrated, and systematically characterized for interoperability, opening the door to new innovations that can avail upon an increased density of within-year and cloud-free observations.

Image geometric and radiometric characterization, long-term archiving, and the generation and validation of analysis ready data products, as exemplified by the Landsat program, are being undertaken by government agencies in recognition of the public good. Simultaneously, rapid advances in commercial cloud computing are accelerating innovation. Determination of the role of the commercial sector and government agencies in Earth observation programs is ongoing. Looking

to the next 50 years, just as in the past, the reliance on governments to fund EO systems and data archives is tenuous. Partnerships between space agencies and commercial satellite providers have been recommended, and are indeed an integral part of current Landsat developments, with commercial building and launching of satellites.

As presented in this paper, incremental improvements and open sharing of the methods and outcomes has empowered an entire scientific and stakeholder community. Open access to high-quality data has resulted in a pronounced scientific impact that has improved understanding of natural and human drivers on the Earth system. These insights have in turn supported policy development and compliance mechanisms. The open availability of Landsat data has enabled nations to benefit from EO data without each one having to build and maintain costly satellite programs. Further, the similarity in data used for national and international monitoring and reporting activity serves to build confidence in outcomes as well as compatibility of the results (i.e., maps, reports) generated. Key thematic areas were presented where high impacts upon a wide range of climatic and societal benefit areas have been realized, thereby demonstrating the breadth of scientific information that can be generated using Landsat data.

Today, building upon the demonstrated utility of Landsat, EO is increasingly recognized as a public good, and an essential part of the critical infrastructure supporting our societies. As enabled and fostered by Landsat, the future of satellite imaging for global terrestrial environmental monitoring is now. As a community, our challenge is no longer obtaining and accessing imagery, but rather acting on the opportunity to convert these data into scientifically-rigorous and societally-relevant information and knowledge.

Dedication

While finalizing this paper, our beloved friend and colleague, Dr. Thomas Loveland, passed away. It is to his memory, we dedicate this work. Tom's vision, leadership, and guidance are behind many of the achievements described in this work. In many ways, Tom's vision became the community vision. He initiated direction, seeded ideas, and encouraged ambition. As long-time Chief Scientist at the USGS EROS Data Center and Co-Chair of the USGS-NASA Landsat Science Team, Tom's vision was amplified and found purchase. Tom was a great friend to many and is sorely missed.

Declaration of Competing Interest

The authors declare that they have no known competing financial interests or personal relationships that could have appeared to influence the work reported in this paper.

Data availability

No data was used for the research described in the article.

Acknowledgements

The Editor and reviewers are thanked for the valuable insights and constructive suggestions made to improve this manuscript. The United States Geological Survey (USGS) and the National Aeronautics and Space Administration (NASA) are gratefully acknowledged for assembly and support of the 2018-2023 Landsat Science Team (https://www.usgs.gov/landsat-missions/landsat-science-teams). Any use of trade, firm, or product names is for descriptive purposes only and does not imply endorsement by the U.S. Government.

References

Anderson, M.C., Neale, C.M.U., Li, F., Norman, J.M., Kustas, W.P., Jayanthi, H., Chavez, J., 2004. Upscaling ground observations of vegetation water content, canopy height, and leaf area index during SMEX02 using aircraft and Landsat imagery. Remote Sens. Environ. 92, 447–464. https://doi.org/10.1016/J.RSE.2004.03.019.

Anderson, M.C., Allen, R.G., Morse, A., Kustas, W.P., 2012. Use of Landsat thermal imagery in monitoring evapotranspiration and managing water resources. Remote Sens. Environ. 122, 50–65. https://doi.org/10.1016/j.rse.2011.08.025.

Aniello, C., Morgan, K., Busbey, A., Newland, L., 1995. Mapping micro-urban heat islands using Landsat TM and a GIS. Comput. Geosci. 21, 965–969. https://doi.org/10.1016/0098-3004(95)00033-5.

Arvidson, T., Gasch, J., Goward, S.N., 2001. Landsat 7's long-term acquisition plan — an innovative approach to building a global imagery archive. Remote Sens. Environ. 78, 13–26. https://doi.org/10.1016/S0034-4257(01)00263-2.

Badhwar, G.D., 1984. Automatic corn-soybean classification using landsat MSS data. I. Near-harvest crop proportion estimation. Remote Sens. Environ. 14, 15–29. https://doi.org/10.1016/0034-4257(84)90004-X.

Ballinger, T., Rohli, R., Allen, M., Robinson, D., Estilow, T., 2018. Half-century perspectives on North American spring snowline and snow cover associations with the Pacific-North American teleconnection pattern. Clim. Res. 74, 201–216. https://doi.org/10.3354/cr01499.

Barsi, J.A., Lee, K., Kvaran, G., Markham, B.L., Pedelty, J.A., 2014. The spectral response of the Landsat-8 operational land imager. Remote Sens. 6, 10232–10251. https://doi.org/10.3390/rs61010232.

Beamish, A., Raynolds, M.K., Epstein, H., Frost, G.V., Macander, M.J., Bergstedt, H., Bartsch, A., Kruse, S., Miles, V., Tanis, C.M., Heim, B., Fuchs, M., Chabrillat, S., Shevtsova, I., Verdonen, M., Wagner, J., 2020. Recent trends and remaining challenges for optical remote sensing of Arctic tundra vegetation: A review and outlook. Remote Sens. Environ. 246, 111872 https://doi.org/10.1016/j.rse.2020.111872.

Beeson, P.C., Daughtry, C.S.T., Wallander, S.A., 2020. Estimates of conservation tillage practices using landsat archive. Remote Sens. 12, 2665. https://doi.org/10.3390/rs12162665.

Bevington, A.R., Menounos, B., 2022. Accelerated change in the glaciated environments of western Canada revealed through trend analysis of optical satellite imagery. Remote Sens. Environ. 270, 112862 https://doi.org/10.1016/j.rse.2021.112862.

Bleyhl, B., Baumann, M., Griffiths, P., Heidelberg, A., Manvelyan, K., Radeloff, V.C., Zazanashvili, N., Kuemmerle, T., 2017. Assessing landscape connectivity for large mammals in the Caucasus using Landsat 8 seasonal image composites. Remote Sens. Environ. 193, 193–203. https://doi.org/10.1016/j.rse.2017.03.001.

Bohn, C.G., Bly, B.G., 1981. Landsat observations of Mount St. Helens. In: Doyle, F.J. (Ed.), Electro-Optical Instrumentation for Resources Evaluation, pp. 32–40. https://doi.org/10.1117/12.931923.

Bolton, D.K., Coops, N.C., Hermosilla, T., Wulder, M.A., White, J.C., Ferster, C.J., 2019. Uncovering regional variability in disturbance trends between parks and greater park ecosystems across Canada (1985–2015). Sci. Rep. 9, 1323. https://doi.org/10.1038/s41598-018-37265-4.

Boryan, C., Yang, Z., Mueller, R., Craig, M., 2011. Monitoring US agriculture: the US Department of Agriculture, National Agricultural Statistics Service, cropland data layer program. Geocarto Int. 26, 341–358. https://doi.org/10.1080/10106049.2011.562309.

Boschetti, L., Roy, D.P., Justice, C.O., Humber, M.L., 2015. MODIS–Landsat fusion for large area 30 m burned area mapping. Remote Sens. Environ. 161, 27–42. https://doi.org/10.1016/j.rse.2015.01.022.

Braaten, J.D., Cohen, W.B., Yang, Z., 2015. Automated cloud and cloud shadow identification in Landsat MSS imagery for temperate ecosystems. Remote Sens. Environ. 169, 128–138. https://doi.org/10.1016/j.rse.2015.08.006.

Brown, J.F., Tollerud, H.J., Barber, C.P., Zhou, Q., Dwyer, J.L., Vogelmann, J.E., Loveland, T.R., Woodcock, C.E., Stehman, S.V., Zhu, Z., Pengra, B.W., Smith, K., Horton, J.A., Xian, G., Auch, R.F., Sohl, T.L., Sayler, K.L., Gallant, A.L., Zelenak, D., Reker, R.R., Rover, J., 2020. Lessons learned implementing an operational continuous United States national land change monitoring capability: the Land Change Monitoring, Assessment, and Projection (LCMAP) approach. Remote Sens. Environ. 238, 111356 https://doi.org/10.1016/j.rse.2019.111356.

Bullock, E.L., Woodcock, C.E., Olofsson, P., 2020a. Monitoring tropical forest degradation using spectral unmixing and Landsat time series analysis. Remote Sens. Environ. 238, 110968 https://doi.org/10.1016/j.rse.2018.11.011.

Bullock, E.L., Woodcock, C.E., Souza, C., Olofsson, P., 2020b. Satellite-based estimates reveal widespread forest degradation in the Amazon. Glob. Chang. Biol. 26, 2956–2969. https://doi.org/10.1111/gcb.15029.

Buma, W., Lee, S.-I., Seo, J., 2018. Recent surface water extent of Lake Chad from multispectral sensors and GRACE. Sensors 18, 2082. https://doi.org/10.3390/s18072082.

Byrne, G.F., Crapper, P.F., Mayo, K.K., 1980. Monitoring land-cover change by principal component analysis of multitemporal landsat data. Remote Sens. Environ. 10, 175–184. https://doi.org/10.1016/0034-4257(80)90021-8.

Carfagna, E., Gallego, F.J., 2006. Using remote sensing for agricultural statistics. Int. Stat. Rev. 73, 389–404. https://doi.org/10.1111/j.1751-5823.2005.tb00155.x.

Caudill, C.E., McArdle, R.C., 1979. Research Evaluation Considerations for AgRISTARS. Department of Agriculture, Economics, Statistics, and Cooperatives Service, Washington, D.C., U.S, 11p.

CBD, 1992. The United Nations Convention on Biological Diversity. Reprinted in International Legal Materials 31 (5 June 1992): 818. (Entered into force 29 December 1993). https://www.cbd.int/doc/legal/cbd-en.pdf.

Chakhar, A., Ortega-Terol, D., Hernández-López, D., Ballesteros, R., Ortega, J.F., Moreno, M.A., 2020. Assessing the accuracy of multiple classification algorithms for crop classification using Landsat-8 and Sentinel-2 data. Remote Sens. 12, 1735. https://doi.org/10.3390/RS12111735.

Chander, G., Markham, B.L., Helder, D.L., 2009. Summary of current radiometric calibration coefficients for Landsat MSS, TM, ETM+, and EO-1 ALI sensors. Remote Sens. Environ. 113, 893–903. https://doi.org/10.1016/j.rse.2009.01.007.

Chavez, P.S., Sides, S.C., Anderson, J.A., 1991. Comparison of three different methods to merge multiresolution and multispectral data: Landsat TM and SPOT panchromatic. Photogramm. Eng. Remote. Sens. 57, 295–303. https://doi.org/10.1306/44b4c288-170a-11d7-8645000102c1865d.

Che, X., Zhang, H.K., Liu, J., 2021. Making Landsat 5, 7 and 8 reflectance consistent using MODIS nadir-BRDF adjusted reflectance as reference. Remote Sens. Environ. 262, 112517 https://doi.org/10.1016/j.rse.2021.112517.

Chen, X.-L., Zhao, H.-M., Li, P.-X., Yin, Z.-Y., 2006. Remote sensing image-based analysis of the relationship between urban heat island and land use/cover changes. Remote Sens. Environ. 104, 133–146. https://doi.org/10.1016/j.rse.2005.11.016.

Chen, J., Chen, J., Liao, A., Cao, X., Chen, L., Chen, X., He, C., Han, G., Peng, S., Lu, M., Zhang, W., Tong, X., Mills, J., 2014. Global land cover mapping at 30m resolution: A POK-based operational approach. ISPRS J. Photogramm. Remote Sens. https://doi.org/10.1016/j.isprsjprs.2014.09.002.

Chen, X., Long, D., Liang, S., He, L., Zeng, C., Hao, X., Hong, Y., 2018a. Developing a composite daily snow cover extent record over the Tibetan Plateau from 1981 to 2016 using multisource data. Remote Sens. Environ. 215, 284–299. https://doi.org/10.1016/j.rse.2018.06.021.

Chen, Y., Lu, D., Luo, L., Pokhrel, Y., Deb, K., Huang, J., Ran, Y., 2018b. Detecting irrigation extent, frequency, and timing in a heterogeneous arid agricultural region using MODIS time series, Landsat imagery, and ancillary data. Remote Sens. Environ. 204, 197–211. https://doi.org/10.1016/j.rse.2017.10.030.

Claverie, M., Ju, J., Masek, J.G., Dungan, J.L., Vermote, E.F., Roger, J.C., Skakun, S.V., Justice, C., 2018. The harmonized Landsat and Sentinel-2 surface reflectance data set. Remote Sens. Environ. 219, 145–161. https://doi.org/10.1016/j.rse.2018.09.002.

Cohen, W.B., Yang, Z., Stehman, S.V., Schroeder, T.A., Bell, D.M., Masek, J.G., Huang, C., Meigs, G.W., 2016. Forest disturbance across the conterminous United States from 1985-2012: the emerging dominance of forest decline. For. Ecol. Manag. 360, 242–252. https://doi.org/10.1016/j.foreco.2015.10.042.

Comber, A.J., Wadsworth, R.A., Fisher, P.F., 2008. Using semantics to clarify the conceptual confusion between land cover and land use : the example of forest. J. Land Use Sci. 3, 185–198. https://doi.org/10.1080/17474230802434187.

Comiso, J.C., Steffen, K., 2001. Studies of Antarctic sea ice concentrations from satellite data and their applications. J. Geophys. Res. Ocean. 106, 31361–31385. https://doi.org/10.1029/2001JC000823.

Connolly, R., Connolly, M., Soon, W., Legates, D., Cionco, R., 2019. Northern hemisphere snow-cover trends (1967–2018): a comparison between climate models and observations. Geosciences 9, 135. https://doi.org/10.3390/geosciences9030135.

Cook, M., Schott, J., Mandel, J., Raqueno, N., 2014. Development of an operational calibration methodology for the Landsat thermal data archive and initial testing of the atmospheric compensation component of a land surface temperature (LST) product from the archive. Remote Sens. 6, 11244–11266. https://doi.org/10.3390/rs61111244.

Coops, N.C., Shang, C., Wulder, M.A., White, J.C., Hermosilla, T., 2020. Change in forest condition: Characterizing non-stand replacing disturbances using time series satellite imagery. For. Ecol. Manag. 474, 118370 https://doi.org/10.1016/j.foreco.2020.118370.

Coppin, P., Jonckheere, I., Nackaerts, K., Muys, B., Lambin, E., 2004. Digital change detection methods in ecosystem monitoring: a review. Int. J. Remote Sens. 25, 1565–1596. https://doi.org/10.1080/0143116031000101675.

Corbane, C., Pesaresi, M., Kemper, T., Politis, P., Florczyk, A.J., Syrris, V., Melchiorri, M., Sabo, F., Soille, P., 2019. Automated global delineation of human settlements from 40 years of Landsat satellite data archives. Big Earth Data 3, 140–169. https://doi.org/10.1080/20964471.2019.1625528.

Cracknell, A.P., 2001. The exciting and totally unanticipated success of the AVHRR in applications for which it was never intended. Adv. Sp. Res. 28, 233–240. https://doi.org/10.1016/S0273-1177(01)00349-0.

DeFries, R., Hansen, A., Newton, A.C., Hansen, M.C., 2005. Increasing isolation of protected areas in tropical forests over the past twenty years. Ecol. Appl. 15, 19–26. https://doi.org/10.1890/03-5258.

Deines, J.M., Kendall, A.D., Hyndman, D.W., 2017. Annual irrigation dynamics in the U. S. northern high plains derived from Landsat satellite data. Geophys. Res. Lett. 44, 9350–9360. https://doi.org/10.1002/2017GL074071.

Doldirina, C., 2015. Open data and Earth observations: the case of opening up access to and use of Earth observation data through the global Earth observation system of systems. J. Intellect. Prop. Inf. Technol. Electron. Commer. Law 6.

Dolman, A.J., Belward, A., Briggs, S., Dowell, M., Eggleston, S., Hill, K., Richter, C., Simmons, A., 2016. A post-Paris look at climate observations. Nat. Geosci. 99 (9), 646. https://doi.org/10.1038/ngeo2785.

Doraiswamy, P.C., Hatfield, J.L., Jackson, T.J., Akhmedov, B., Prueger, J., Stern, A., 2004. Crop condition and yield simulations using Landsat and MODIS. Remote Sens. Environ. 92, 548–559. https://doi.org/10.1016/j.rse.2004.05.017.

Dozier, J., Marks, D., 1987. Snow mapping and classification from Landsat thematic mapper data. Ann. Glaciol. 9, 97–103. https://doi.org/10.3189/s026030550000046x.

Drusch, M., Del Bello, U., Carlier, S., Colin, O., Fernandez, V., Gascon, F., Hoersch, B., Isola, C., Laberinti, P., Martimort, P., Meygret, A., Spoto, F., Sy, O., Marchese, F., Bargellini, P., 2012. Sentinel-2: ESA's optical high-resolution mission for GMES operational services. Remote Sens. Environ. 120, 25–36. https://doi.org/10.1016/j.rse.2011.11.026.

Duro, D.C., Coops, N.C., Wulder, M.A., Han, T., 2007. Development of a large area biodiversity monitoring system driven by remote sensing. Prog. Phys. Geogr. 31, 235–260. https://doi.org/10.1177/0309133307079054.

Duro, D.C., Girard, J., King, D.J., Fahrig, L., Mitchell, S., Lindsay, K., Tischendorf, L., 2014. Predicting species diversity in agricultural environments using Landsat TM imagery. Remote Sens. Environ. 144, 214–225. https://doi.org/10.1016/j.rse.2014.01.001.

Dwyer, J.L., Roy, D.P., Sauer, B., Jenkerson, C.B., Zhang, H.K., Lymburner, L., 2018. Analysis ready data: enabling analysis of the Landsat archive. Remote Sens. 10, 1363. https://doi.org/10.3390/rs10091363.

Echeverria, C., Coomes, D., Salas, J., Rey-Benayas, J.M., Lara, A., Newton, A., 2006. Rapid deforestation and fragmentation of Chilean Temperate Forests. Biol. Conserv. 130, 481–494. https://doi.org/10.1016/j.biocon.2006.01.017.

Ellis, E.C., 2021. Land use and ecological change: A 12,000-year history. Annu. Rev. Environ. Resour. 46, 1–33. https://doi.org/10.1146/annurev-environ-012220-010822.

Elmes, A., Levy, C., Erb, A., Hall, D.K., Scambos, T.A., DiGirolamo, N., Schaaf, C., 2021. Consequences of the 2019 greenland ice sheet melt episode on Albedo. Remote Sens. 13, 227. https://doi.org/10.3390/rs13020227.

Fahnestock, M., Scambos, T., Moon, T., Gardner, A., Haran, T., Klinger, M., 2016. Rapid large-area mapping of ice flow using Landsat 8. Remote Sens. Environ. 185, 84–94. https://doi.org/10.1016/j.rse.2015.11.023.

Farwell, L.S., Gudex-Cross, D., Anise, I.E., Bosch, M.J., Olah, A.M., Radeloff, V.C., Razenkova, E., Rogova, N., Silveira, E.M.O., Smith, M.M., Pidgeon, A.M., 2021. Satellite image texture captures vegetation heterogeneity and explains patterns of bird richness. Remote Sens. Environ. 253, 112175 https://doi.org/10.1016/j.rse.2020.112175.

Foody, G.M., Palubinskas, G., Lucas, R.M., Curran, P.J., Honzak, M., 1996. Identifying terrestrial carbon sinks: classification of successional stages in regenerating tropical forest from Landsat TM data. Remote Sens. Environ. 55, 205–216. https://doi.org/10.1016/S0034-4257(95)00196-4.

Franz, B.A., Bailey, S.W., Kuring, N., Werdell, P.J., 2015. Ocean color measurements with the Operational Land Imager on Landsat-8: implementation and evaluation in SeaDAS. J. Appl. Remote. Sens. 9, 096070 https://doi.org/10.1117/1.JRS.9.096070.

Fraser, R.S., Kaufman, Y.J., 1985. The relative importance of aerosol scattering and absorption in remote sensing. IEEE Trans. Geosci. Remote Sens. GE-23, 625–633. https://doi.org/10.1109/TGRS.1985.289380.

Friedl, M.A., McIver, D.K., Hodges, J.C.F., Zhang, X.Y., Muchoney, D., Strahler, A.H., Woodcock, C.E., Gopal, S., Schneider, A., Cooper, A., Baccini, A., Gao, F., Schaaf, C., 2002. Global land cover mapping from MODIS: algorithms and early results. Remote Sens. Environ. 83, 287–302. https://doi.org/10.1016/S0034-4257(02)00078-0.

Fritz, S., See, L., McCallum, I., You, L., Bun, A., Moltchanova, E., Duerauer, M., Albrecht, F., Schill, C., Perger, C., Havlik, P., Mosnier, A., Thornton, P., Wood-Sichra, U., Herrero, M., Becker-Reshef, I., Justice, C., Hansen, M., Gong, P., Abdel Aziz, S., Cipriani, A., Cumani, R., Cecchi, G., Conchedda, G., Ferreira, S., Gomez, A., Haffani, M., Kayitakire, F., Malanding, J., Mueller, R., Newby, T., Nonguierma, A., Olusegun, A., Ortner, S., Rajak, D.R., Rocha, J., Schepaschenko, D., Schepaschenko, M., Terekhov, A., Tiangwa, A., Vancutsem, C., Vintrou, E., Wenbin, W., Velde, M., Dunwoody, A., Kraxner, F., Obersteiner, M., 2015. Mapping global cropland and field size. Glob. Chang. Biol. 21, 1980–1992. https://doi.org/10.1111/gcb.12838.

Frost, G.V., Epstein, H.E., Walker, D.A., 2014. Regional and landscape-scale variability of Landsat-observed vegetation dynamics in northwest Siberian tundra. Environ. Res. Lett. 9, 025004 https://doi.org/10.1088/1748-9326/9/2/025004.

Gao, F., Masek, J., Schwaller, M., Hall, F., 2006. On the blending of the landsat and MODIS surface reflectance: Predicting daily landsat surface reflectance. IEEE Trans. Geosci. Remote Sens. 44, 2207–2218. https://doi.org/10.1109/TGRS.2006.872081.

Gao, F., Anderson, M.C., Zhang, X., Yang, Z., Alfieri, J.G., Kustas, W.P., Mueller, R., Johnson, D.M., Prueger, J.H., 2017. Toward mapping crop progress at field scales through fusion of Landsat and MODIS imagery. Remote Sens. Environ. 188, 9–25. https://doi.org/10.1016/j.rse.2016.11.004.

Gardner, A.S., Moholdt, G., Scambos, T., Fahnstock, M., Ligtenberg, S., Van Den Broeke, M., Nilsson, J., 2018. Increased West Antarctic and unchanged East Antarctic ice discharge over the last 7 years. Cryosphere 12, 521–547. https://doi.org/10.5194/tc-12-521-2018.

Gardner, A.S., Fahnestock, M.A., Scambos, T.A., 2022. MEaSUREs ITS_LIVE Landsat Image-Pair Glacier and Ice Sheet Surface Velocities: Version 1. [WWW Document]. https://doi.org/10.5067/IMR9D3PEI28U.

Gascon, F., Bouzinac, C., Thépaut, O., Jung, M., Francesconi, B., Louis, J., Lonjou, V., Lafrance, B., Massera, S., Gaudel-Vacaresse, A., Languille, F., Alhammoud, B., Viallefont, F., Pflug, B., Bieniarz, J., Clerc, S., Pessiot, L., Trémas, T., Cadau, E., De Bonis, R., Isola, C., Martimort, P., Fernandez, V., 2017. Copernicus Sentinel-2A calibration and products validation status. Remote Sens. 9, 584. https://doi.org/10.3390/rs9060584.

GCOS, 2016. The Global Observing System for Climate: Implementation Needs. World Meteorological Organisation. Geneva. GCOS-200. 341p. https://gcos.wmo.int/en/gcos-implementation-plan.

Gerace, A., Kleynhans, T., Eon, R., Montanaro, M., 2020. Towards an operational, split window-derived surface temperature product for the thermal infrared sensors onboard Landsat 8 and 9. Remote Sens. 12, 224. https://doi.org/10.3390/rs12020224.

Gibbs, H.K., Brown, S., Niles, J.O., Foley, J.A., 2007. Monitoring and estimating tropical forest carbon stocks: making REDD a reality. Environ. Res. Lett. 2, 045023 https://doi.org/10.1088/1748-9326/2/4/045023.

Gibbs, H.K., Ruesch, A.S., Achard, F., Clayton, M.K., Holmgren, P., Ramankutty, N., Foley, J.A., 2010. Tropical forests were the primary sources of new agricultural land

in the 1980s and 1990s. Proc. Natl. Acad. Sci. 107, 16732–16737. https://doi.org/10.1073/pnas.0910275107.
Giri, C., Ochieng, E., Tieszen, L.L., Zhu, Z., Singh, A., Loveland, T., Masek, J., Duke, N., 2011. Status and distribution of mangrove forests of the world using earth observation satellite data. Glob. Ecol. Biogeogr. 20, 154–159. https://doi.org/10.1111/j.1466-8238.2010.00584.x.
Gitelson, A.A., Peng, Y., Masek, J.G., Rundquist, D.C., Verma, S., Suyker, A., Baker, J.M., Hatfield, J.L., Meyers, T., 2012. Remote estimation of crop gross primary production with Landsat data. Remote Sens. Environ. 121, 404–414. https://doi.org/10.1016/j.rse.2012.02.017.
Giuliani, G., Chatenoux, B., De Bono, A., Rodila, D., Richard, J.-P., Allenbach, K., Dao, H., Peduzzi, P., 2017. Building an Earth Observations Data Cube: lessons learned from the Swiss Data Cube (SDC) on generating Analysis Ready Data (ARD). Big Earth Data 1, 100–117. https://doi.org/10.1080/20964471.2017.1398903.
Gong, P., Wang, J., Yu, L., Zhao, Yongchao, Zhao, Yuanyuan, Liang, L., Niu, Z., Huang, X., Fu, H., Liu, S., Li, C., Li, X., Fu, W., Liu, C., Xu, Y., Wang, X., Cheng, Q., Hu, L., Yao, W., Zhang, Han, Zhu, P., Zhao, Z., Zhang, Haiying, Zheng, Y., Ji, L., Zhang, Y., Chen, H., Yan, A., Guo, J., Yu, Liang, Wang, L., Liu, X., Shi, T., Zhu, M., Chen, Y., Yang, G., Tang, P., Xu, B., Giri, C., Clinton, N., Zhu, Z., Chen, Jin, Chen, Jun, 2013. Finer resolution observation and monitoring of global land cover: first mapping results with Landsat TM and ETM+ data. Int. J. Remote Sens. 34, 2607–2654. https://doi.org/10.1080/01431161.2012.748992.
Gong, P., Li, X., Wang, J., Bai, Y., Chen, B., Hu, T., Liu, X., Xu, B., Yang, J., Zhang, W., Zhou, Y., 2020. Annual maps of global artificial impervious area (GAIA) between 1985 and 2018. Remote Sens. Environ. 236, 111510 https://doi.org/10.1016/J.RSE.2019.111510.
Gordon, S.I., 1980. Utilizing LANDSAT imagery to monitor land-use change: a case study in ohio. Remote Sens. Environ. 9, 189–196. https://doi.org/10.1016/0034-4257(80)90028-0.
Gordon, H.R., Clark, D.K., 1981. Clear water radiances for atmospheric correction of coastal zone color scanner imagery. Appl. Opt. 20, 4175. https://doi.org/10.1364/AO.20.004175.
Gorelick, N., Hancher, M., Dixon, M., Ilyushchenko, S., Thau, D., Moore, R., 2017. Google Earth Engine: planetary-scale geospatial analysis for everyone. Remote Sens. Environ. 202, 18–27. https://doi.org/10.1016/j.rse.2017.06.031.
Goward, S.N., 1989. Satellite bioclimatology. J. Clim. 2, 710–720. https://doi.org/10.1175/1520-0442(1989)002<0710:sb>2.0.co;2.
Goward, S., Williams, D., 1997. Landsat and earth systems science: development of terrestrial monitoring. Photogramm. Eng. Remote. Sens. 63, 887–900.
Goward, S.N., Williams, D.L., Arvidson, T., Rocchio, L.E.P., Irons, J.R., Russell, C.A., Johnston, S.S., 2017. Landsat's Enduring Legacy: Pioneering Global Land Observations from Space. American Society for Photogrammetry and Remote Sensing, Bethesda, MD. ISBN-10: 1570831017. 586p.
Goward, S.N., Masek, J.G., Loveland, T.R., Dwyer, J.L., Williams, D.L., Arvidson, T., Corp, L.M., Rocchio, L.E.P., Irons, J.R., 2021. Semi-centennial of Landsat observations & pending Landsat 9 launch. Photogramm. Eng. Remote. Sens. 87, 1–7. https://doi.org/10.14358/PERS.87.8.1.
Gross, G., Helder, D., Begeman, C., Leigh, L., Kaewmanee, M., Shah, R., 2022. Initial cross-calibration of Landsat 8 and Landsat 9 using the simultaneous underfly event. Remote Sens. 14, 2418. https://doi.org/10.3390/rs14102418.
Haack, B., Bryant, N., Adams, S., 1987. An assessment of landsat MSS and TM data for urban and near-urban land-cover digital classification. Remote Sens. Environ. 21, 201–213. https://doi.org/10.1016/0034-4257(87)90053-8.
Hakimdavar, R., Hubbard, A., Policelli, F., Pickens, A., Hansen, M., Fatoyinbo, T., Lagomasino, D., Pahlevan, N., Unninayar, S., Kavvada, A., Carroll, M., Smith, B., Hurwitz, M., Wood, D., Schollaert Uz, S., 2020. Monitoring water-related ecosystems with Earth observation data in support of sustainable development goal (SDG) 6 reporting. Remote Sens. 12, 1634. https://doi.org/10.3390/rs12101634.
Hall, F., Badhwar, G., 1987. Signature-extendable technology: global space-based crop recognition. IEEE Trans. Geosci. Remote Sens. GE-25, 93–103. https://doi.org/10.1109/TGRS.1987.289785.
Hall, F., Botkin, D., Strebel, D., Woods, K.S.G., 1991. Large-scale patterns of forest succession as determined by remote sensing. Ecol. 72, 628–640.
Hansen, M.C., Loveland, T.R., 2012. A review of large area monitoring of land cover change using Landsat data. Remote Sens. Environ. 122, 66–74. https://doi.org/10.1016/j.rse.2011.08.024.
Hansen, M., Franklin, S., Woudsma, C., Peterson, M., 2001. Caribou habitat mapping and fragmentation analysis using Landsat MSS, TM, and GIS data in the North Columbia Mountains, British Columbia, Canada. Remote Sens. Environ. 77, 50–65. https://doi.org/10.1016/S0034-4257(01)00193-6.
Hansen, M.C., Potapov, P.V., Moore, R., Hancher, M., Turubanova, S.A., Tyukavina, A., Thau, D., Stehman, S.V., Goetz, S.J., Loveland, T.R., Kommareddy, A., Egorov, A., Chini, L., Justice, C.O., Townshend, J.R.G., 2013. High-resolution global maps of 21st-century forest cover change. Science (80-.) 342, 850–853. https://doi.org/10.1126/science.1244693.
Hansen, M.C., Potapov, P.V., Pickens, A.H., Tyukavina, A., Hernandez-Serna, A., Zalles, V., Turubanova, S., Kommareddy, I., Stehman, S.V., Song, X., Kommareddy, A., 2022. Global land use extent and dispersion within natural land cover using Landsat data. Environ. Res. Lett. 17, 034050 https://doi.org/10.1088/1748-9326/ac46ec.
He, K.S., Bradley, B.A., Cord, A.F., Rocchini, D., Tuanmu, M., Schmidtlein, S., Turner, W., Wegmann, M., Pettorelli, N., 2015. Will remote sensing shape the next generation of species distribution models? Remote Sens. Ecol. Conserv. 1, 4–18. https://doi.org/10.1002/rse2.7.
Healey, S.P., Yang, Z., Cohen, W.B., Pierce, D.J., 2006. Application of two regression-based methods to estimate the effects of partial harvest on forest structure using Landsat data. Remote Sens. Environ. 101, 115–126.
Healey, S.P., Cohen, W.B., Yang, Z., Kenneth Brewer, C., Brooks, E.B., Gorelick, N., Hernandez, A.J., Huang, C., Joseph Hughes, M., Kennedy, R.E., Loveland, T.R., Moisen, G.G., Schroeder, T.A., Stehman, S.V., Vogelmann, J.E., Woodcock, C.E., Yang, L., Zhu, Z., 2018. Mapping forest change using stacked generalization: an ensemble approach. Remote Sens. Environ. 204, 717–728. https://doi.org/10.1016/j.rse.2017.09.029.
Healey, S.P., Yang, Z., Gorelick, N., Ilyushchenko, S., 2020. Highly local model calibration with a new GEDI LiDAR asset on Google Earth engine reduces landsat forest height signal saturation. Remote Sens. 12, 2840. https://doi.org/10.3390/rs12172840.
Hermosilla, T., Wulder, M.A., White, J.C., Coops, N.C., Hobart, G.W., 2015a. Regional detection, characterization, and attribution of annual forest change from 1984 to 2012 using Landsat-derived time-series metrics. Remote Sens. Environ. 170, 121–132. https://doi.org/10.1016/j.rse.2015.09.004.
Hermosilla, T., Wulder, M.A., White, J.C., Coops, N.C., Hobart, G.W., 2015b. An integrated Landsat time series protocol for change detection and generation of annual gap-free surface reflectance composites. Remote Sens. Environ. 158, 220–234. https://doi.org/10.1016/j.rse.2014.11.005.
Hermosilla, T., Wulder, M.A., White, J.C., Coops, N.C., Hobart, G.W., Campbell, L.B., 2016. Mass data processing of time series Landsat imagery: pixels to data products for forest monitoring. Int. J. Digit. Earth 9, 1035–1054. https://doi.org/10.1080/17538947.2016.1187673.
Hermosilla, T., Wulder, M.A., White, J.C., Coops, N.C., Hobart, G.W., 2018. Disturbance-informed annual land cover classification maps of Canada's forested ecosystems for a 29-year Landsat time series. Can. J. Remote. Sens. 44, 67–87. https://doi.org/10.1080/07038992.2018.1437719.
Hermosilla, T., Wulder, M.A., White, J.C., Coops, N.C., Pickell, P.D., Bolton, D.K., 2019. Impact of time on interpretations of forest fragmentation: three-decades of fragmentation dynamics over Canada. Remote Sens. Environ. 222, 65–77. https://doi.org/10.1016/j.rse.2018.12.027.
Hermosilla, T., Wulder, M.A., White, J.C., Coops, N.C., 2022. Land cover classification in an era of big and open data: optimizing localized implementation and training data selection to improve mapping outcomes. Remote Sens. Environ. 268, 112780 https://doi.org/10.1016/j.rse.2021.112780.
Hilker, T., Wulder, M.A., Coops, N.C., Linke, J., McDermid, G., Masek, J.G., Gao, F., White, J.C., 2009. A new data fusion model for high spatial- and temporal-resolution mapping of forest disturbance based on Landsat and MODIS. Remote Sens. Environ. 113, 1613–1627. https://doi.org/10.1016/j.rse.2009.03.007.
Hoffman, J., Ackerman, S., Liu, Y., Key, J., 2019. The detection and characterization of Arctic Sea ice leads with satellite imagers. Remote Sens. 11, 521. https://doi.org/10.3390/rs11050521.
Holden, C.E., Woodcock, C.E., 2016. An analysis of Landsat 7 and Landsat 8 underflight data and the implications for time series investigations. Remote Sens. Environ. 185, 16–36. https://doi.org/10.1016/j.rse.2016.02.052.
Homer, C.G., Edwards, T.C., Ramsey, R.D., Price, K.P., 1993. Use of remote sensing methods in modelling sage grouse winter habitat. J. Wildl. Manag. 57, 78. https://doi.org/10.2307/3809003.
Homer, C., Huang, C., Yang, L., Wylie, B., Coan, M., 2004. Development of a 2001 national land-cover database for the United States. Photogramm. Eng. Remote. Sens. 70, 829–840. https://doi.org/10.14358/PERS.70.7.829.
Homer, C., Dewitz, J., Yang, L., Jin, S., Danielson, P., Xian, G., Coulston, J., Herold, N., Wickham, J., Megown, K., 2015. Completion of the 2011 national land cover database for the conterminous United States – representing a decade of land cover change information. Photogramm. Eng. Remote. Sens. 81, 345–354. https://doi.org/10.1016/S0099-1112(15)30100-2.
Hu, T., Yang, J., Li, X., Gong, P., He, Y., Weng, Q., Koch, M., Thenkabail, P.S., 2016. Mapping urban land use by using landsat images and open social data. Remote Sens. 8, 151, 2016. 8, 151. https://doi.org/10.3390/RS8020151.
Hu, Q., Xiang, M., Chen, D., Zhou, J., Wu, W., Song, Q., 2020. Global cropland intensification surpassed expansion between 2000 and 2010: a spatio-temporal analysis based on GlobeLand30. Sci. Total Environ. 746, 141035 https://doi.org/10.1016/j.scitotenv.2020.141035.
Huang, C., Goward, S.N., Masek, J.G., Thomas, N., Zhu, Z., Vogelmann, J.E., 2010. An automated approach for reconstructing recent forest disturbance history using dense Landsat time series stacks. Remote Sens. Environ. 114, 183–198. https://doi.org/10.1016/j.rse.2009.08.017.
Huete, A.R., Liu, H.Q., Batchily, K., Van Leeuwen, W., 1997. A comparison of vegetation indices over a global set of TM images for EOS-MODIS. Remote Sens. Environ. 59, 440–451. https://doi.org/10.1016/S0034-4257(96)00112-5.
Hufbauer, K., 1991. The Landsat case. Science (80-.) 254, 314. https://doi.org/10.1126/science.254.5029.314.
Hulley, G.C., Hook, S.J., Abbott, E., Malakar, N., Islam, T., Abrams, M., 2015. The ASTER Global Emissivity Dataset (ASTER GED): mapping Earth's emissivity at 100 meter spatial scale. Geophys. Res. Lett. 42, 7966–7976. https://doi.org/10.1002/2015GL065564.
IPCC, 2019. Climate Change and Land: an IPCC special report on climate change, desertification, land degradation, sustainable land management, food security, and greenhouse gas fluxes in terrestrial ecosystems, P.R. Shukla [Lead editor], 874p. https://www.ipcc.ch/srccl/.
IPCC, 2021. Summary for Policymakers. In: Climate Change 2021: The Physical Science Basis. Contribution of Working Group I to the Sixth Assessment Report of the Intergovernmental Panel on Climate Change, V. Masson-Delmotte [Lead editor], 3949p. https://www.ipcc.ch/re.

Jackson, T.J., Chen, D., Cosh, M., Li, F., Anderson, M., Walthall, C., Doriaswamy, P., Hunt, E.R., 2004. Vegetation water content mapping using Landsat data derived normalized difference water index for corn and soybeans. Remote Sens. Environ. 92, 475–482. https://doi.org/10.1016/j.rse.2003.10.021.

Jacobs, J.D., Simms, É.L., Simms, A., 1997. Recession of the southern part of Barnes Ice Cap, Baffin Island, Canada, between 1961 and 1993, determined from digital mapping of Landsat TM. J. Glaciol. 43, 98–102. https://doi.org/10.3189/S0022143000002859.

Johnson, D.M., 2019. Using the Landsat archive to map crop cover history across the United States. Remote Sens. Environ. 232, 111286 https://doi.org/10.1016/j.rse.2019.111286.

Johnson, D.M., Mueller, R., 2010. The 2009 cropland data layer. Photogramm. Eng. Remote. Sens. 76, 1201–1205.

Joughin, I., Smith, B.E., Howat, I., 2018. Greenland Ice Mapping Project: Ice flow velocity variation at sub-monthly to decadal timescales. Cryosphere 12, 2211–2227. https://doi.org/10.5194/tc-12-2211-2018.

Ju, J., Masek, J.G., 2016. The vegetation greenness trend in Canada and US Alaska from 1984-2012 Landsat data. Remote Sens. Environ. 176, 1–16. https://doi.org/10.1016/j.rse.2016.01.001.

Justice, C.O., Vermote, E., Townshend, J.R.G., Defries, R., Roy, D.P., Hall, D.K., Salomonson, V.V., Privette, J.L., Riggs, G., Strahler, A., Lucht, W., Myneni, R.B., Knyazikhin, Y., Running, S.W., Nemani, R.R., Wan, Z., Huete, A.R., Van Leeuwen, W., Wolfe, R.E., Giglio, L., Muller, J.P., Lewis, P., Barnsley, M.J., 1998. The moderate resolution imaging spectroradiometer (MODIS): Land remote sensing for global change research. IEEE Trans. Geosci. Remote Sens. 36, 1228–1249. https://doi.org/10.1109/36.701075.

Justice, C., Townshend, J.R., Vermote, E., Masuoka, E., Wolfe, R., Saleous, N., Roy, D., Morisette, J., 2002. An overview of MODIS Land data processing and product status. Remote Sens. Environ. 83, 3–15. https://doi.org/10.1016/S0034-4257(02)00084-6.

Kauth, R., Thomas, G., 1976. The Tasselled Cap – A Graphic Description of the Spectral-Temporal Development of Agricultural Crops as Seen by LANDSAT. In: LARS Symposia, Paper 159. https://docs.lib.purdue.edu/lars_symp/159/.

Kennedy, R.E., Yang, Z., Cohen, W.B., 2010. Detecting trends in forest disturbance and recovery using yearly Landsat time series: 1. LandTrendr — Temporal segmentation algorithms. Remote Sens. Environ. 114, 2897–2910. https://doi.org/10.1016/j.rse.2010.07.008.

Kennedy, R.E., Yang, Z., Cohen, W.B., Pfaff, E., Braaten, J., Nelson, P., 2012. Spatial and temporal patterns of forest disturbance and regrowth within the area of the Northwest Forest Plan. Remote Sens. Environ. 122, 117–133. https://doi.org/10.1016/j.rse.2011.09.024.

Kennedy, R.E., Andréfouët, S., Cohen, W.B., Gómez, C., Griffiths, P., Hais, M., Healey, S.P., Helmer, E.H., Hostert, P., Lyons, M.B., Meigs, G.W., Pflugmacher, D., Phinn, S.R., Powell, S.L., Scarth, P., Sen, S., Schroeder, T.A., Schneider, A., Sonnenschein, R., Vogelmann, J.E., Wulder, M.A., Zhu, Z., 2014. Bringing an ecological view of change to landsat-based remote sensing. Front. Ecol. Environ. 12, 339–346. https://doi.org/10.1890/130066.

Kennedy, R.E., Yang, Z., Braaten, J., Copass, C., Antonova, N., Jordan, C., Nelson, P., 2015. Attribution of disturbance change agent from Landsat time-series in support of habitat monitoring in the Puget Sound region, USA. Remote Sens. Environ. 166, 271–285. https://doi.org/10.1016/j.rse.2015.05.005.

Kern, S., Lavergne, T., Pedersen, L.T., Tonboe, R.T., Bell, L., Meyer, M., Zeigermann, L., 2022. Satellite passive microwave sea-ice concentration data set intercomparison using Landsat data. Cryosph. 16, 349–378. https://doi.org/10.5194/tc-16-349-2022.

King, L.A., Adusei, B., Stehman, S.V., Potapov, P.V., Song, X.P., Krylov, A., Di Bella, C., Loveland, T.R., Johnson, D.M., Hansen, M.C., 2017. A multi-resolution approach to national-scale cultivated area estimation of soybean. Remote Sens. Environ. 195, 13–29. https://doi.org/10.1016/j.rse.2017.03.047.

Kingslake, J., Ely, J.C., Das, I., Bell, R.E., 2017. Widespread movement of meltwater onto and across Antarctic ice shelves. Nature 544, 349–352. https://doi.org/10.1038/nature22049.

Kuemmerle, T., Erb, K., Meyfroidt, P., Müller, D., Verburg, P.H., Estel, S., Haberl, H., Hostert, P., Jepsen, M.R., Kastner, T., Levers, C., Lindner, M., Plutzar, C., Verkerk, P.J., van der Zanden, E.H., Reenberg, A., 2013. Challenges and opportunities in mapping land use intensity globally. Curr. Opin. Environ. Sustain. 5, 484–493. https://doi.org/10.1016/j.cosust.2013.06.002.

Lambin, E.F., Turner, B.L., Geist, H.J., Agbola, S.B., Angelsen, A., Bruce, J.W., Coomes, O.T., Dirzo, R., Fischer, G., Folke, C., George, P.S., Homewood, K., Imbernon, J., Leemans, R., Li, X., Moran, E.F., Mortimore, M., Ramakrishnan, P.S., Richards, J.F., Skånes, H., Steffen, W., Stone, G.D., Svedin, U., Veldkamp, T.A., Vogel, C., Xu, J., 2001. The causes of land-use and land-cover change: moving beyond the myths. Glob. Environ. Chang. 11, 261–269. https://doi.org/10.1016/S0959-3780(01)00007-3.

Laraby, K.G., Schott, J.R., 2018. Uncertainty estimation method and Landsat 7 global validation for the Landsat surface temperature product. Remote Sens. Environ. 216, 472–481. https://doi.org/10.1016/j.rse.2018.06.026.

Lawrence, R.L., Ripple, W.J., 2000. Fifteen years of revegetation of Mount St. Helens: a landscape-scale analysis. Ecology 81, 2742–2752. https://doi.org/10.1890/0012-9658(2000)081[2742:FYOROM]2.0.CO;2.

Leimgruber, P., Christen, C.A., Laborderie, A., 2005. The impact of Landsat satellite monitoring on conservation biology. Environ. Monit. Assess. 106, 81–101. https://doi.org/10.1007/s10661-005-0763-0.

Li, J., Chen, B., 2020. Global revisit interval analysis of Landsat-8 -9 and Sentinel-2A -2B data for terrestrial monitoring. Sensors 20, 6631. https://doi.org/10.3390/s20226631.

Li, J., Roy, D.P., 2017. A global analysis of Sentinel-2A, Sentinel-2B and Landsat-8 data revisit intervals and implications for terrestrial monitoring. Remote Sens. 9, 902. https://doi.org/10.3390/rs9090902.

Li, Z., Sun, W., Zeng, Q., 1998. Measurements of Glacier variation in the Tibetan plateau using Landsat data. Remote Sens. Environ. 63, 258–264. https://doi.org/10.1016/S0034-4257(97)00140-5.

Lindquist, E., D'Annunzio, R., 2016. Assessing global forest land-use change by object-based image analysis. Remote Sens. 8, 678. https://doi.org/10.3390/rs8080678.

Liu, J., Linderman, M., Ouyang, Z., An, L., Yang, J., Zhang, H., 2001. Ecological degradation in protected areas: the case of Wolong nature reserve for giant pandas. Science. 292 (5514), 98–101. https://doi.org/10.1126/science.1058104.

Liu, Z., He, C., Zhou, Y., Wu, J., 2014. How much of the world's land has been urbanized, really? A hierarchical framework for avoiding confusion. Landsc. Ecol. 29, 763–771. https://doi.org/10.1007/s10980-014-0034-y.

Liu, Y., Hill, M.J., Zhang, X., Wang, Z., Richardson, A.D., Hufkens, K., Filippa, G., Baldocchi, D.D., Ma, S., Verfaillie, J., Schaaf, C.B., 2017. Using data from Landsat, MODIS, VIIRS and PhenoCams to monitor the phenology of California oak/grass savanna and open grassland across spatial scales. Agric. For. Meteorol. 237–238, 311–325. https://doi.org/10.1016/j.agrformet.2017.02.026.

Liu, X., Hu, G., Chen, Y., Li, X., Xu, X., Li, S., Pei, F., Wang, S., 2018. High-resolution multi-temporal mapping of global urban land using Landsat images based on the Google Earth Engine Platform. Remote Sens. Environ. 209, 227–239. https://doi.org/10.1016/J.RSE.2018.02.055.

MacDonald, R.B., 1984. A summary of the history of the development of automated remote sensing for agricultural applications. IEEE Trans. Geosci. Remote Sens. GE-22, 473–482. https://doi.org/10.1109/TGRS.1984.6499157.

MacDonald, R.B., Hall, F.G., 1980. Global Crop Forecasting. Science (80-.) 208, 670–679. https://doi.org/10.1126/SCIENCE.208.4445.670.

MacDonald, R.B., Hall, F.G., Erb, R.B., 1975. "The Use of LANDSAT Data in a Large Area Crop Inventory Experiment (LACIE)" In LARS Symposia, Paper 46. http://docs.lib.purdue.edu/lars_symp/46.

Mack, P., 1990. Viewing the Earth: The Social Construction of the Landsat Satellite System. MIT Press, Cambridge, Mass.

Malakar, N.K., Hulley, G.C., Hook, S.J., Laraby, K., Cook, M., Schott, J.R., 2018. An operational land surface temperature product for Landsat thermal data: methodology and validation. IEEE Trans. Geosci. Remote Sens. 56, 5717–5735. https://doi.org/10.1109/TGRS.2018.2824828.

Markham, B.L., Helder, D.L., 2012. Forty-year calibrated record of earth-reflected radiance from Landsat: a review. Remote Sens. Environ. 122, 30–40. https://doi.org/10.1016/j.rse.2011.06.026.

Markham, B.L., Arvidson, T., Barsi, J.A., Choate, M., Kaita, E., Levy, R., Lubke, M., Masek, J.G., 2018. Landsat program. In: Comprehensive Remote Sensing. Elsevier, pp. 27–90. https://doi.org/10.1016/B978-0-12-409548-9.10313-6.

Markham, B.L., Anderson, C., Choate, M., Crawford, C., Jenstrom, D., Masek, J., Pedelty, J., Sauer, B., Thome, K., 2021. Landsat 9: ready for launch. In: Butler, J.J., Xiong, X. (Jack), Gu, X. (Eds.), Earth Observing Systems XXVI. SPIE, p. 26. https://doi.org/10.1117/12.2595885.

Markus, T., Cavalieri, D.J., Tschudi, M.A., Ivanoff, A., 2003. Comparison of aerial video and Landsat 7 data over ponded sea ice. Remote Sens. Environ. 86, 458–469. https://doi.org/10.1016/S0034-4257(03)00124-X.

Marshall, E., 1989. Landsat: Cliff-hanging, again. Science (80-.) 246, 1–4. https://doi.org/10.1126/science.246.4928.321-b.

Masek, J.G., Vermote, E.F., Saleous, N.E., Wolfe, R., Hall, F.G., Huemmrich, K.F., Gao, F., Kutler, J., Lim, T.-K., 2006. A Landsat surface reflectance dataset for North America, 1990–2000. IEEE Geosci. Remote Sens. Lett. 3, 68–72. https://doi.org/10.1109/LGRS.2005.857030.

Masek, J.G., Wulder, M.A., Markham, B., McCorkel, J., Crawford, C.J., Storey, J., Jenstrom, D.T., 2020. Landsat 9: empowering open science and applications through continuity. Remote Sens. Environ. 248, 111968 https://doi.org/10.1016/j.rse.2020.111968.

Matasci, G., Hermosilla, T., Wulder, M.A., White, J.C., Coops, N.C., Hobart, G.W., Bolton, D.K., Tompalski, P., Bater, C.W., 2018. Three decades of forest structural dynamics over Canada's forested ecosystems using Landsat time-series and lidar plots. Remote Sens. Environ. 216, 697–714. https://doi.org/10.1016/j.rse.2018.07.024.

McCorkel, J., McAndrew, B., Barsi, J., Markham, B., Pharr, J., Rodriguez, M., Shuman, T., Sushkov, A., Zukowski, B., 2019. First results from laser-based spectral characterization of Landsat 9 operational land imager-2. In: IGARSS 2019–2019 IEEE International Geoscience and Remote Sensing Symposium. IEEE, pp. 9044–9047. https://doi.org/10.1109/IGARSS.2019.8898508.

Melton, F.S., Huntington, J., Grimm, R., Herring, J., Hall, M., Rollison, D., Erickson, T., Allen, R., Anderson, M., Fisher, J.B., Kilic, A., Senay, G.B., Volk, J., Hain, C., Johnson, L., Ruhoff, A., Blankenau, P., Bromley, M., Carrara, W., Daudert, B., Doherty, C., Dunkerly, C., Friedrichs, M., Guzman, A., Halverson, G., Hansen, J., Harding, J., Kang, Y., Ketchum, D., Minor, B., Morton, C., Ortega-Salazar, S., Ott, T., Ozdogan, M., ReVelle, P.M., Schull, M., Wang, C., Yang, Y., Anderson, R.G., 2021. OpenET: filling a critical data gap in water management for the Western United States. JAWRA J. Am. Water Resour. Assoc. 1–24 https://doi.org/10.1111/1752-1688.12956.

Moussavi, M., Pope, A., Halberstadt, A., Trusel, L., Cioffi, L., Abdalati, W., 2020. Antarctic supraglacial lake detection using Landsat 8 and Sentinel-2 imagery: towards continental generation of lake volumes. Remote Sens. 12, 134. https://doi.org/10.3390/rs12010134.

Nagendra, H., Lucas, R., Honrado, J.P., Jongman, R.H.G., Tarantino, C., Adamo, M., Mairota, P., 2013. Remote sensing for conservation monitoring: assessing protected

areas, habitat extent, habitat condition, species diversity, and threats. Ecol. Indic. 33, 45–59. https://doi.org/10.1016/j.ecolind.2012.09.014.
National Research Council, 2013. Landsat and beyond: Sustaining and enhancing the Nation's Land Imaging Program, Landsat and Beyond: Sustaining and Enhancing the Nation's Land Imaging Program. The National Academies Press, Washington, DC. https://doi.org/10.17226/18420.
Nunez, J., Otazu, X., Fors, O., Prades, A., Pala, V., Arbiol, R., 1999. Multiresolution-based image fusion with additive wavelet decomposition. IEEE Trans. Geosci. Remote Sens. 37, 1204–1211. https://doi.org/10.1109/36.763274.
Odum, E.P., 1969. The strategy of ecosystem development. Science (80-.) 164, 262–270. https://doi.org/10.1126/science.164.3877.262.
OECD, 2020. Cities in the World : A New Perspective on Urbanisation, 171p. https://www.oecd-ilibrary.org/urban-rural-and-regional-development/cities-in-the-world_d0efcbda-en.
Ouma, Y.O., Tateishi, R., 2006. A water index for rapid mapping of shoreline changes of five East African Rift Valley lakes: an empirical analysis using Landsat TM and ETM+ data. Int. J. Remote Sens. 27, 3153–3181. https://doi.org/10.1080/01431160500309934.
Pahlevan, N., Schott, J.R., Franz, B.A., Zibordi, G., Markham, B., Bailey, S., Schaaf, C.B., Ondrusek, M., Greb, S., Strait, C.M., 2017. Landsat 8 remote sensing reflectance (Rrs) products: evaluations, intercomparisons, and enhancements. Remote Sens. Environ. 190, 289–301. https://doi.org/10.1016/j.rse.2016.12.030.
Pahlevan, N., Mangin, A., Balasubramanian, S.V., Smith, B., Alikas, K., Arai, K., Barbosa, C., Bélanger, S., Binding, C., Bresciani, M., Giardino, C., Gurlin, D., Fan, Y., Harmel, T., Hunter, P., Ishikaza, J., Kratzer, S., Lehmann, M.K., Ligi, M., Ma, R., Martin-Lauzer, F.R., Olmanson, L., Oppelt, N., Pan, Y., Peters, S., Reynaud, N., Sander de Carvalho, L.A., Simis, S., Spyrakos, E., Steinmetz, F., Stelzer, K., Sterckx, S., Tormos, T., Tyler, A., Vanhellemont, Q., Warren, M., 2021. ACIX-Aqua: a global assessment of atmospheric correction methods for Landsat-8 and Sentinel-2 over lakes, rivers, and coastal waters. Remote Sens. Environ. 258, 112366 https://doi.org/10.1016/J.RSE.2021.112366.
Painter, T.H., Skiles, S.M.K., Deems, J.S., Brandt, W.T., Dozier, J., 2018. Variation in rising limb of colorado river snowmelt runoff hydrograph controlled by dust radiative forcing in snow. Geophys. Res. Lett. 45, 797–808. https://doi.org/10.1002/2017GL075826.
Park, S.H., Lee, M.J., Jung, H.S., 2016. Spatiotemporal analysis of snow cover variations at Mt. Kilimanjaro using multi-temporal Landsat images during 27 years. J. Atmos. Solar-Terrestrial Phys. 143–144, 37–46. https://doi.org/10.1016/j.jastp.2016.03.007.
Pekel, J.F., Cottam, A., Gorelick, N., Belward, A.S., 2016. High-resolution mapping of global surface water and its long-term changes. Nature 540, 418–422. https://doi.org/10.1038/nature20584.
Pérez-Hoyos, A., Rembold, F., Kerdiles, H., Gallego, J., 2017. Comparison of global land cover datasets for cropland monitoring. Remote Sens. 9, 1118. https://doi.org/10.3390/rs9111118.
Pesaresi, M., Ehrlich, D., Ferri, S., Florczyk, A.J., Freire, S., Halkia, M., Julea, A., Kemper, T., Soille, P., Syrris, V., 2016. Operating procedure for the production of the Global Human Settlement Layer from Landsat data of the epochs 1975, 1990, 2000, and 2014. EUR 27741. Publications Office of the European Union, Luxembourg (Luxembourg). https://doi.org/10.2788/253582.
Pettorelli, N., Owen, H.J.F., Duncan, C., 2016. How do we want Satellite Remote Sensing to support biodiversity conservation globally? Methods Ecol. Evol. 7, 656–665. https://doi.org/10.1111/2041-210X.12545.
Pickens, A.H., Hansen, M.C., Hancher, M., Stehman, S.V., Tyukavina, A., Potapov, P., Marroquin, B., Sherani, Z., 2020. Mapping and sampling to characterize global inland water dynamics from 1999 to 2018 with full Landsat time-series. Remote Sens. Environ. 243, 111792 https://doi.org/10.1016/j.rse.2020.111792.
Pitts, D.E., Badhwar, G., 1980. Field size, length, and width distributions based on LACIE ground truth data. Remote Sens. Environ. 10, 201–213. https://doi.org/10.1016/0034-4257(80)90024-3.
Potapov, P., Li, X., Hernandez-Serna, A., Tyukavina, A., Hansen, M.C., Kommareddy, A., Pickens, A., Turubanova, S., Tang, H., Silva, C.E., Armston, J., Dubayah, R., Blair, J. B., Hofton, M., 2021. Mapping global forest canopy height through integration of GEDI and Landsat data. Remote Sens. Environ. 253, 112165 https://doi.org/10.1016/j.rse.2020.112165.
Potapov, P., Turubanova, S., Hansen, M.C., Tyukavina, A., Zalles, V., Khan, A., Song, X. P., Pickens, A., Shen, Q., Cortez, J., 2022. Global maps of cropland extent and change show accelerated cropland expansion in the twenty-first century. Nat. Food 3, 19–28. https://doi.org/10.1038/s43016-021-00429-z.
Qiu, S., Zhu, Z., Shang, R., Crawford, C.J., 2021. Can Landsat 7 preserve its science capability with a drifting orbit? Sci. Remote Sens. 4, 100026 https://doi.org/10.1016/j.srs.2021.100026.
Rickbeil, G.J.M., Coops, N.C., Berman, E.E., McClelland, C.J.R., Bolton, D.K., Stenhouse, G.B., 2020. Changing spring snow cover dynamics and early season forage availability affect the behavior of a large carnivore. Glob. Chang. Biol. 26, 6266–6275. https://doi.org/10.1111/gcb.15295.
Rosenthal, W., Dozier, J., 1996. Automated mapping of montane snow cover at subpixel resolution from the Landsat thematic mapper. Water Resour. Res. 32, 115–130. https://doi.org/10.1029/95WR02718.
Roy, D.P., Ju, J., Mbow, C., Frost, P., Loveland, T., 2010. Accessing free Landsat data via the Internet: Africa's challenge. Remote Sens. Lett. 1, 111–117. https://doi.org/10.1080/01431160903486693.
Roy, D.P., Qin, Y., Kovalskyy, V., Vermote, E.F., Ju, J., Egorov, A., Hansen, M.C., Kommareddy, I., Yan, L., 2014a. Conterminous United States demonstration and characterization of MODIS-based Landsat ETM+ atmospheric correction. Remote Sens. Environ. 140, 433–449. https://doi.org/10.1016/j.rse.2013.09.012.
Roy, D.P., Wulder, M.A., Loveland, T.R., Woodcock, C.E., Allen, R.G., Anderson, M.C., Helder, D., Irons, J.R., Johnson, D.M., Kennedy, R., Scambos, T.A., Schaaf, C.B., Schott, J.R., Sheng, Y., Vermote, E.F., Belward, A.S., Bindschadler, R., Cohen, W.B., Gao, F., Hipple, J.D., Hostert, P., Huntington, J., Justice, C.O., Kilic, A., Kovalskyy, V., Lee, Z.P., Lymburner, L., Masek, J.G., McCorkel, J., Shuai, Y., Trezza, R., Vogelmann, J., Wynne, R.H., Zhu, Z., 2014b. Landsat-8: Science and product vision for terrestrial global change research. Remote Sens. Environ. 145, 154–172. https://doi.org/10.1016/j.rse.2014.02.001.
Roy, D.P., Kovalskyy, V., Zhang, H.K., Vermote, E.F., Yan, L., Kumar, S.S., Egorov, A., 2016a. Characterization of Landsat-7 to Landsat-8 reflective wavelength and normalized difference vegetation index continuity. Remote Sens. Environ. 185, 57–70. https://doi.org/10.1016/j.rse.2015.12.024.
Roy, D.P., Zhang, H.K., Ju, J., Gomez-Dans, J.L., Lewis, P.E., Schaaf, C.B., Sun, Q., Li, J., Huang, H., Kovalskyy, V., 2016b. A general method to normalize Landsat reflectance data to nadir BRDF adjusted reflectance. Remote Sens. Environ. 176, 255–271. https://doi.org/10.1016/j.rse.2016.01.023.
Roy, D.P., Li, J., Zhang, H.K., Yan, L., Huang, H., Li, Z., 2017. Examination of Sentinel-2A multi-spectral instrument (MSI) reflectance anisotropy and the suitability of a general method to normalize MSI reflectance to nadir BRDF adjusted reflectance. Remote Sens. Environ. 199, 25–38. https://doi.org/10.1016/j.rse.2017.06.019.
Rudorff, A.F., Batista, G.T., 1991. Wheat yield estimation at the farm level using tm landsat and agrometeorological data. Int. J. Remote Sens. 12, 2477–2484. https://doi.org/10.1080/01431169108955281.
Saarinen, N., White, J., Wulder, M., Kangas, A., Tuominen, S., Kankare, V., Holopainen, M., Hyyppä, J., Vastaranta, M., 2018. Landsat archive holdings for Finland: opportunities for forest monitoring. Silva Fenn. 52 https://doi.org/10.14214/sf.9986.
Sala, O.E., Stuart Chapin III, F., Armesto, J.J., Berlow, E., Bloomfield, J., Dirzo, R., Huber-Sanwald, E., Huenneke, L.F., Jackson, R.B., Kinzig, A., Leemans, R., Lodge, D. M., Mooney, H.A., Oesterheld, M., Poff, N.L., Sykes, M.T., Walker, B.H., Walker, M., Wall, D.H., 2000. Global Biodiversity Scenarios for the Year 2100. Science (80-.) 287, 1770–1774. https://doi.org/10.1126/science.287.5459.1770.
Sanderson, E.W., Jaiteh, M., Levy, M.A., Redford, K.H., Wannebo, A.V., Woolmer, G., 2002. The human footprint and the last of the wild. Bioscience 52, 891–904. https://doi.org/10.1641/0006-3568(2002)052[0891:THFATL]2.0.CO;2.
Scambos, T.A., Dutkiewicz, M.J., Wilson, J.C., Bindschadler, R.A., 1992. Application of image cross-correlation to the measurement of glacier velocity using satellite image data. Remote Sens. Environ. 42, 177–186. https://doi.org/10.1016/0034-4257(92)90101-O.
Schneibel, A., Stellmes, M., Röder, A., Frantz, D., Kowalski, B., Haß, E., Hill, J., 2017. Assessment of spatio-temporal changes of smallholder cultivation patterns in the Angolan Miombo belt using segmentation of Landsat time series. Remote Sens. Environ. 195, 118–129. https://doi.org/10.1016/j.rse.2017.04.012.
Schneider, S.R., McGinnis, D.F., Stephens, G., 1985. Monitoring Africa's lake chad basin with LANDSAT and NOAA satellite data. Int. J. Remote Sens. 6, 59–73. https://doi.org/10.1080/01431168508948424.
Scott, J.M., Davis, F., Csuti, B., Noss, R., Butterfield, B., Anderson, H., Caicco, S., Erchia, F.D., Edwards, T.C., Ulliman, J., 1993. Gap analysis: a geographic approach to protection of biological diversity. Wildl. Monogr. 123, 3–41. https://www.jstor.org/stable/3830788.
Seehaus, T., Malz, P., Sommer, C., Lippl, S., Cochachin, A., Braun, M., 2019. Changes of the tropical glaciers throughout Peru between 2000 and 2016 - Mass balance and area fluctuations. Cryosphere 13, 2537–2556. https://doi.org/10.5194/tc-13-2537-2019.
Selkowitz, D.J., Forster, R.R., 2016. Automated mapping of persistent ice and snow cover across the western U.S. with Landsat. ISPRS J. Photogramm. Remote Sens. 117, 126–140. https://doi.org/10.1016/j.isprsjprs.2016.04.001.
Senay, G.B., Friedrichs, M., Morton, C., Parrish, G.E.L., Schauer, M., Khand, K., Kagone, S., Boiko, O., Huntington, J., 2022. Mapping actual evapotranspiration using Landsat for the conterminous United States: Google Earth Engine implementation and assessment of the SSEBop model. Remote Sens. Environ. 275, 113011 https://doi.org/10.1016/j.rse.2022.113011.
Seto, K.C., Woodcock, C.E., Song, C., Huang, X., Lu, J., Kaufmann, R.K., 2002. Monitoring land-use change in the Pearl River Delta using Landsat TM. Int. J. Remote Sens. 23, 1985–2004. https://doi.org/10.1080/01431160110075532.
Sieber, A., Kuemmerle, T., Prishchepov, A.V., Wendland, K.J., Baumann, M., Radeloff, V. C., Baskin, L.M., Hostert, P., 2013. Landsat-based mapping of post-Soviet land-use change to assess the effectiveness of the Oksky and Mordovsky protected areas in European Russia. Remote Sens. Environ. 133, 38–51. https://doi.org/10.1016/J.RSE.2013.01.021.
Skakun, S., Wevers, J., Brockmann, C., Doxani, G., Aleksandrov, M., Batič, M., Frantz, D., Gascon, F., Gómez-Chova, L., Hagolle, O., López-Puigdollers, D., Louis, J., Lubej, M., Mateo-García, G., Osman, J., Peressutti, D., Pflug, B., Puc, J., Richter, R., Roger, J.-C., Scaramuzza, P., Vermote, E., Vesel, N., Zupanc, A., Žust, L., 2022. Cloud Mask Intercomparison eXercise (CMIX): An evaluation of cloud masking algorithms for Landsat 8 and Sentinel-2. Remote Sens. Environ. 274, 112990 https://doi.org/10.1016/j.rse.2022.112990.
Skole, D., Tucker, C., 1993. Tropical deforestation and habitat fragmentation in the Amazon: satellite data from 1978 to 1988. Science (80-.) 260, 1905–1910. https://doi.org/10.1126/science.260.5116.1905.
Sommer, S., Zucca, C., Grainger, A., Cherlet, M., Zougmore, R., Sokona, Y., Hill, J., Della Peruta, R., Roehrig, J., Wang, G., 2011. Application of indicator systems for monitoring and assessment of desertification from national to global scales. L. Degrad. Dev. 22, 184–197. https://doi.org/10.1002/LDR.1084.

Song, C., Woodcock, C.E., Seto, K.C., Lenney, M.P., Macomber, S.A., 2001. Classification and change detection using Landsat TM data. Remote Sens. Environ. 75, 230–244. https://doi.org/10.1016/S0034-4257(00)00169-3.

Song, X.P., Potapov, P.V., Krylov, A., King, L.A., Di Bella, C.M., Hudson, A., Khan, A., Adusei, B., Stehman, S.V., Hansen, M.C., 2017. National-scale soybean mapping and area estimation in the United States using medium resolution satellite imagery and field survey. Remote Sens. Environ. 190, 383–395. https://doi.org/10.1016/j.rse.2017.01.008.

Steffen, K., Heinrichs, J., 1994. Feasibility of sea ice typing with synthetic aperture radar (SAR): merging of Landsat thematic mapper and ERS 1 SAR satellite imagery. J. Geophys. Res. 99, 22413. https://doi.org/10.1029/94jc01398.

St-Louis, V., Pidgeon, A.M., Clayton, M.K., Locke, B.A., Bash, D., Radeloff, V.C., 2009. Satellite image texture and a vegetation index predict avian biodiversity in the Chihuahuan Desert of New Mexico. Ecography (Cop.). 32, 468–480. https://doi.org/10.1111/j.1600-0587.2008.05512.x.

Storey, J., Choate, M., Lee, K., 2014. Landsat 8 Operational Land Imager On-Orbit Geometric Calibration and Performance. Remote Sens. 6, 11127–11152. https://doi.org/10.3390/rs61111127.

Storey, J.C., Rengarajan, R., Choate, M.J., 2019. Bundle adjustment using space-based triangulation method for improving the Landsat global ground reference. Remote Sens. 11, 1–25. https://doi.org/10.3390/rs11141640.

Tang, X., Hutyra, L.R., Arévalo, P., Baccini, A., Woodcock, C.E., Olofsson, P., 2020. Spatiotemporal tracking of carbon emissions and uptake using time series analysis of Landsat data: a spatially explicit carbon bookkeeping model. Sci. Total Environ. 720, 137409 https://doi.org/10.1016/j.scitotenv.2020.137409.

Thenkabail, P.S., Ward, A.D., Lyon, J.G., 1994. Landsat-5 thematic mapper models of soybean and corn crop characteristics. Int. J. Remote Sens. 15, 49–61. https://doi.org/10.1080/01431169408954050.

Townshend, J.R., 1992. Land cover. Int. J. Remote Sens. 13, 1319–1328. https://doi.org/10.1080/01431169208904193.

Trefois, P., 1995. Monitoring the evolution of desertification processes from 1973 to 1987 in Damagaram (Niger) with Landsat multispectral scanner and thematic mapper. In: Mougin, E., Ranson, K.J., Smith, J.A. (Eds.), Multispectral and Microwave Sensing of Forestry, Hydrology, and Natural Resources. SPIE, pp. 383–396. https://doi.org/10.1117/12.200778.

Tulbure, M.G., Hostert, P., Kuemmerle, T., Broich, M., 2021. Regional matters: On the usefulness of regional land-cover datasets in times of global change. Remote Sens. Ecol. Conserv. 1–12 https://doi.org/10.1002/rse2.248.

Turner, W., Spector, S., Gardiner, N., Fladeland, M., Sterling, E., Steininger, M., 2003. Remote sensing for biodiversity science and conservation. Trends Ecol. Evol. 18, 306–314. https://doi.org/10.1016/S0169-5347(03)00070-3.

Turner, W., Rondinini, C., Pettorelli, N., Mora, B., Leidner, A.K., Szantoi, Z., Buchanan, G., Dech, S., Dwyer, J., Herold, M., Koh, L.P., Leimgruber, P., Taubenboeck, H., Wegmann, M., Wikelski, M., Woodcock, C., 2015. Free and open-access satellite data are key to biodiversity conservation. Biol. Conserv. 182, 173–176. https://doi.org/10.1016/j.biocon.2014.11.048.

Turubanova, S., Potapov, P.V., Tyukavina, A., Hansen, M.C., 2018. Ongoing primary forest loss in Brazil, Democratic Republic of the Congo, and Indonesia. Environ. Res. Lett. 13, 074028 https://doi.org/10.1088/1748-9326/AACD1C.

UNESG, 2020. Report of the Inter-Agency and Expert Group on SDG Indicators. Proceedings of the Economic and Social Council. https://tcg.uis.unesco.org/wp-content/uploads/sites/4/2020/10/TCG-7-REF-1.pdf.

Venter, O., Sanderson, E.W., Magrach, A., Allan, J.R., Beher, J., Jones, K.R., Possingham, H.P., Laurance, W.F., Wood, P., Fekete, B.M., Levy, M.A., Watson, J.E. M., 2016. Sixteen years of change in the global terrestrial human footprint and implications for biodiversity conservation. Nat. Commun. 7, 12558. https://doi.org/10.1038/ncomms12558.

Vermote, E., Justice, C., Claverie, M., Franch, B., 2015. Preliminary analysis of the performance of the Landsat 8/OLI land surface reflectance product. Remote Sens. Environ. 185, 46–56. https://doi.org/10.1016/j.rse.2016.04.008.

Vogelmann, J.E., Howard, S.M., Yang, L., Larson, C.R., Wylie, B.K., VanDriel, N., 2001. Completion of the 1990s national land cover data set for the conterminous United States from Landsat Thematic Mapper Data and Ancillary Data Sources. Photogramm. Eng. Remote. Sens. (June), 650–662.

Vogelmann, J.E., Gallant, A.L., Shi, H., Zhu, Z., 2015. Perspectives on monitoring gradual change across the continuity of Landsat sensors using time-series data. Remote Sens. Environ. 185, 258–270. https://doi.org/10.1016/j.rse.2016.02.060.

Wang, Z., Schaaf, C.B., Sun, Q., Kim, J., Erb, A.M., Gao, F., Román, M.O., Yang, Y., Petroy, S., Taylor, J.R., Masek, J.G., Morisette, J.T., Zhang, X., Papuga, S.A., 2017. Monitoring land surface albedo and vegetation dynamics using high spatial and temporal resolution synthetic time series from Landsat and the MODIS BRDF/NBAR/albedo product. Int. J. Appl. Earth Obs. Geoinf. 59, 104–117. https://doi.org/10.1016/j.jag.2017.03.008.

Weise, K., Höfer, R., Franke, J., Guelmami, A., Simonson, W., Muro, J., O'Connor, B., Strauch, A., Flink, S., Eberle, J., Mino, E., Thulin, S., Philipson, P., van Valkengoed, E., Truckenbrodt, J., Zander, F., Sánchez, A., Schröder, C., Thonfeld, F., Fitoka, E., Scott, E., Ling, M., Schwarz, M., Kunz, I., Thürmer, G., Plasmeijer, A., Hilarides, L., 2020. Wetland extent tools for SDG 6.6.1 reporting from the Satellite-based Wetland Observation Service (SWOS). Remote Sens. Environ. 247, 111892 https://doi.org/10.1016/j.rse.2020.111892.

Welch, R., Pannell, C.W., Lo, C.P., 1975. Land use in Northeast China, 1973: a view from Landsat-1. Ann. Assoc. Am. Geogr. 65, 595–596. https://doi.org/10.1111/j.1467-8306.1975.tb01067.x.

Weng, Q., Lu, D., Schubring, J., 2004. Estimation of land surface temperature–vegetation abundance relationship for urban heat island studies. Remote Sens. Environ. 89, 467–483. https://doi.org/10.1016/j.rse.2003.11.005.

White, J.C., Wulder, M.A., Hermosilla, T., Coops, N.C., Hobart, G.W., 2017. A nationwide annual characterization of 25 years of forest disturbance and recovery for Canada using Landsat time series. Remote Sens. Environ. 194, 303–321. https://doi.org/10.1016/j.rse.2017.03.035.

White, J.C., Wulder, M.A., Hermosilla, T., Coops, N.C., 2019. Satellite time series can guide forest restoration. Nature 569, 630. https://doi.org/10.1038/d41586- 019-01665-x.

White, J.C., Hermosilla, T., Wulder, M.A., Coops, N.C., 2022. Mapping, validating, and interpreting spatio-temporal trends in post-disturbance forest recovery. Remote Sens. Environ. 271, 112904 https://doi.org/10.1016/j.rse.2022.112904.

Williams, D.L., Miller, L.D., 1979. Monitoring Forest Canopy Alteration Around the World with Digital Analysis of Landsat Data. NASA.

Williams, R.S., Ferrigno, J.G., Kent, T.M., Schoonmaker, J.W., 1982. Landsat images and mosaics of antarctica for mapping and glaciological studies. Ann. Glaciol. 3, 321–326. https://doi.org/10.3189/S0260305500003001.

Williams, R.S., Ferrigno, J.G., Swithinbank, C., Lucchitta, B.K., Seekins, B.A., 1995. Coastal-change and glaciological maps of Antarctica. Ann. Glaciol. 21, 284–290. https://doi.org/10.3189/S0260305500015950.

Winkler, K., Fuchs, R., Rounsevell, M., Herold, M., 2021. Global land use changes are four times greater than previously estimated. Nat. Commun. 12, 2501. https://doi.org/10.1038/s41467-021-22702-2.

Woodcock, C.E., Allen, R., Anderson, M., Belward, A., Bindschadler, R., Cohen, W., Gao, F., Goward, S.N., Helder, D., Helmer, E., Nemani, R., Oreopoulos, L., Schott, J., Thenkabail, P.S., Vermote, E.F., Vogelmann, J., Wulder, M.A., Wynne, R., 2008. Free access to Landsat imagery. Science (80-.) 320, 1011. https://doi.org/10.1126/science.320.5879.1011a.

Woodcock, C.E., Loveland, T.R., Herold, M., Bauer, M.E., 2020. Transitioning from change detection to monitoring with remote sensing: a paradigm shift. Remote Sens. Environ. 238, 111558 https://doi.org/10.1016/j.rse.2019.111558.

Wu, Z., Snyder, G., Vadnais, C., Arora, R., Babcock, M., Stensaas, G., Doucette, P., Newman, T., 2019. User needs for future Landsat missions. Remote Sens. Environ. 231, 111214 https://doi.org/10.1016/j.rse.2019.111214.

Wulder, M.A., Coops, N.C., 2014. Satellites: Make Earth observations open access. Nature 513, 30–31. https://doi.org/10.1038/513030a.

Wulder, M.A., Masek, J.G., Cohen, W.B., Loveland, T.R., Woodcock, C.E., 2012. Opening the archive: How free data has enabled the science and monitoring promise of Landsat. Remote Sens. Environ. 122, 2–10. https://doi.org/10.1016/j.rse.2012.01.010.

Wulder, M.A., Hilker, T., White, J.C., Coops, N.C., Masek, J.G., Pflugmacher, D., Crevier, Y., 2015. Virtual constellations for global terrestrial monitoring. Remote Sens. Environ. 170, 62–76. https://doi.org/10.1016/j.rse.2015.09.001.

Wulder, M.A., White, J.C., Loveland, T.R., Woodcock, C.E., Belward, A.S., Cohen, W.B., Fosnight, E.A., Shaw, J., Masek, J.G., Roy, D.P., 2016. The global Landsat archive: Status, consolidation, and direction. Remote Sens. Environ. 185, 271–283. https://doi.org/10.1016/j.rse.2015.11.032.

Wulder, M.A., Coops, N.C., Roy, D.P., White, J.C., Hermosilla, T., 2018. Land cover 2.0. Int. J. Remote Sens. 39, 4254–4284. https://doi.org/10.1080/01431161.2018.1452075.

Wulder, M.A., Loveland, T.R., Roy, D.P., Crawford, C.J., Masek, J.G., Woodcock, C.E., Allen, R.G., Anderson, M.C., Belward, A.S., Cohen, W.B., Dwyer, J., Erb, A., Gao, F., Griffiths, P., Helder, D., Hermosilla, T., Hipple, J.D., Hostert, P., Hughes, M.J., Huntington, J., Johnson, D.M., Kennedy, R., Kilic, A., Li, Z., Lymburner, L., McCorkel, J., Pahlevan, N., Scambos, T.A., Schaaf, C., Schott, J.R., Sheng, Y., Storey, J., Vermote, E., Vogelmann, J., White, J.C., Wynne, R.H., Zhu, Z., 2019. Current status of Landsat program, science, and applications. Remote Sens. Environ. 225, 127–147. https://doi.org/10.1016/j.rse.2019.02.015.

Xian, G., Homer, C., Fry, J., 2009. Updating the 2001 National Land Cover Database land cover classification to 2006 by using Landsat imagery change detection methods. Remote Sens. Environ. 113, 1133–1147. https://doi.org/10.1016/j.rse.2009.02.004.

Xu, H., 2006. Modification of normalised difference water index (NDWI) to enhance open water features in remotely sensed imagery. Int. J. Remote Sens. 27, 3025–3033. https://doi.org/10.1080/01431160600589179.

Yamazaki, D., Trigg, M.A., Ikeshima, D., 2015. Development of a global ~90m water body map using multi-temporal Landsat images. Remote Sens. Environ. 171, 337–351. https://doi.org/10.1016/j.rse.2015.10.014.

Yan, L., Roy, D.P., 2016. Conterminous United States crop field size quantification from multi-temporal Landsat data. Remote Sens. Environ. 172, 67–86. https://doi.org/10.1016/j.rse.2015.10.034.

Yan, L., Roy, D.P., 2021. Improving Landsat Multispectral Scanner (MSS) geolocation by least-squares-adjustment based time-series co-registration. Remote Sens. Environ. 252, 112181 https://doi.org/10.1016/j.rse.2020.112181.

Yang, Y., Anderson, M.C., Gao, F., Wood, J.D., Gu, L., Hain, C., 2021. Studying drought-induced forest mortality using high spatiotemporal resolution evapotranspiration data from thermal satellite imaging. Remote Sens. Environ. 265, 112640 https://doi.org/10.1016/j.rse.2021.112640.

Yuan, F., Bauer, M.E., 2007. Comparison of impervious surface area and normalized difference vegetation index as indicators of surface urban heat island effects in Landsat imagery. Remote Sens. Environ. 106, 375–386. https://doi.org/10.1016/j.rse.2006.09.003.

Zalles, V., Hansen, M.C., Potapov, P.V., Parker, D., Stehman, S.V., Pickens, A.H., Parente, L.L., Ferreira, L.G., Song, X.P., Hernandez-Serna, A., Kommareddy, I., 2021. Rapid expansion of human impact on natural land in South America since 1985. Sci. Adv. 7 https://doi.org/10.1126/sciadv.abg1620.

Zhang, H.K., Roy, D.P., 2016. Landsat 5 Thematic Mapper reflectance and NDVI 27-year time series inconsistencies due to satellite orbit change. Remote Sens. Environ. 186, 217–233. https://doi.org/10.1016/j.rse.2016.08.022.

Zheng, B., Campbell, J.B., de Beurs, K.M., 2012. Remote sensing of crop residue cover using multi-temporal Landsat imagery. Remote Sens. Environ. 117, 177–183. https://doi.org/10.1016/j.rse.2011.09.016.

Zhu, Z., 2017. Change detection using landsat time series: A review of frequencies, preprocessing, algorithms, and applications. ISPRS J. Photogramm. Remote Sens. 130, 370–384. https://doi.org/10.1016/j.isprsjprs.2017.06.013.

Zhu, Z., Woodcock, C.E., 2012. Object-based cloud and cloud shadow detection in Landsat imagery. Remote Sens. Environ. 118, 83–94. https://doi.org/10.1016/j.rse.2011.10.028.

Zhu, Z., Woodcock, C.E., 2014. Continuous change detection and classification of land cover using all available Landsat data. Remote Sens. Environ. 144, 152–171. https://doi.org/10.1016/j.rse.2014.01.011.

Zhu, Z., Wang, S., Woodcock, C.E., 2015. Improvement and expansion of the Fmask algorithm: cloud, cloud shadow, and snow detection for Landsats 4–7, 8, and Sentinel 2 images. Remote Sens. Environ. 159, 269–277. https://doi.org/10.1016/j.rse.2014.12.014.

Zhu, Z., Wulder, M.A., Roy, D.P., Woodcock, C.E., Hansen, M.C., Radeloff, V.C., Healey, S.P., Schaaf, C., Hostert, P., Strobl, P., Pekel, J.-F., Lymburner, L., Pahlevan, N., Scambos, T.A., 2019a. Benefits of the free and open Landsat data policy. Remote Sens. Environ. 224, 382–385. https://doi.org/10.1016/j.rse.2019.02.016.

Zhu, Z., Zhou, Y., Seto, K.C., Stokes, E.C., Deng, C., Pickett, S.T.A., Taubenböck, H., 2019b. Understanding an urbanizing planet: Strategic directions for remote sensing. Remote Sens. Environ. 228, 164–182. https://doi.org/10.1016/j.rse.2019.04.020.